ACS Chemical Neuroscience

Thiazolyl-thiadiazines as BACE-1 Inhibitors and Anti-inflammatory Agents: Multitarget-Directed Ligands for the Efficient Management of Alzheimer's Disease

Sneha Sagar, Devendra Pratap Singh, Nirupa B Panchal, Rajesh D Das, Dhaivat H Pandya, Vasudevan Sudarsanam, Manish Nivsarkar, and Kamala K. Vasu

ACS Chem. Neurosci., **Just Accepted Manuscript** • DOI: 10.1021/acschemneuro.8b00063 • Publication Date (Web): 26 Apr 2018

Thiazolyl-thiadiazines as BACE-1 Inhibitors and Anti-inflammatory Agents: Multitarget-Directed Ligands for the Efficient Management of Alzheimer's Disease[**]

Sneha R. Sagar[a,c], Devendra Pratap Singh[b], Nirupa B. Panchal[a,c], Rajesh D. Das[a], Dhaivat H. Pandya[a], Vasudevan Sudarsanam[a], Manish Nivsarkar[b], Kamala K. Vasu[a*]

[a]Department of Medicinal Chemistry, B. V. Patel Pharmaceutical Education and Research Development (PERD) Centre, S. G. Highway, Thaltej, Ahmedabad-380054, Gujarat, India

[b]Department of Pharmacology and Toxicology, B. V. Patel Pharmaceutical Education and Research Development (PERD) Centre, S. G. Highway, Thaltej, Ahmedabad-380054, Gujarat, India

[c]Institute of Pharmacy, NIRMA University, S. G. Highway, Chandlodia, Gota, Ahmedabad-382481, Gujarat, India

*Corresponding author. Tel.: + 91 79 27439375; Fax: + 91 79 27450449

E-mail: kamkva@gmail.com, kamalav@perdcentre.com

[#]Communication Ref. No.: PERD95012018

Abstract:

Alzheimer's disease (AD) is associated with multiple neuropathological events including BACE-1 inhibition and neuronal inflammation, ensuing degeneracy and death to neuronal cells. Targeting such a complex disease *via* a single target directed treatment was found to be inefficacious. Hence, with an intention to incorporate multiple therapeutic effects within a single molecule; multitarget-directed ligands (MTDLs) have been evolved. Herein, for the first time we report the discovery of novel thiazolyl-thiadiazines which can serve as MTDLs as evident from the *in vitro* and *in vivo* studies. These MTDLs exhibited BACE-1 inhibition down to micromolar

range and results from the in *vivo* studies demonstrated efficient anti-inflammatory activity with inherent gastro-intestinal safety. Moreover, compound **6d** unveiled noteworthy anti-oxidant, anti-amyloid, neuroprotective, and anti-amnesic properties. Overall, results of the present study manifest the potential outcome of thiazolyl-thiadiazines for AD treatment.

Keywords: Drug discovery, BACE-1, Inflammation, Multitarget-directed ligands

Introduction:

Alzheimer's disease (AD) is a progressive degenerative neurological disorder of the brain. The two widely accepted hallmarks of AD pathogenesis are amyloid plaques and neurofibrillary tangles. Certain other factors that affect the pathophysiology of this disorder are inflammation, neurotransmitter imbalance, oxidative stress and rising cholesterol levels.[1] Currently, the available drugs treat only behavioral and cognitive symptoms related to this disease but none of them are applicable for disease modifying treatment of AD.[2] As a result, there is an unmet need to develop anti-amyloid drugs in order to combat complex AD pathogenesis. In recent years, BACE-1 (Beta site APP cleaving enzyme-1) has emerged as one of the main targets for AD intervention. BACE-1 is the key enzyme of amyloidogenic cascade that acts on amyloid precursor protein (APP) and eventually helps in formation of amyloid plaques in the extracellular site.[3] Despite being the prime target of AD, preclinical BACE-1 inhibitors have failed so far to show promising efficacy during clinical studies.[4] Therefore, it can be presumed that AD treatment interferes with more than one neuropathological mechanism simultaneously. In this context, multitarget-directed ligands (MTDLs) have emerged as an effective approach for disease modifying AD treatment and proven to be advantageous over single target anti-amyloid therapy.[5] Amyloid plaques induces the release of various inflammatory cytokines like TNF-α, IL-1β and cyclooxygenases (COXs).[6] Therefore, neuronal inflammation is considered to be the downstream factor for AD pathogenesis. The collaborative influence of BACE-1 and neuronal inflammation lead to neuronal cell degeneration and cell death.[7]

Broadly speaking, the MTDLs are compounds which endow ability to interact with multiple biological targets simultaneously. Besides, they reduce the pharmacokinetic and drug-drug interaction problems linked to multiple-medication therapy and generally show a synergistic

effect. The design and development of new MTDLs seems to be an attractive and widely adopted approach in AD drug discovery, as attested by numerous researchers around the globe. Certain examples of MTDLs are: dual BACE-1 and acetylcholinesterase (AChE) inhibitors, dual BACE-1 and glycogen synthase kinase (GSK)-3β inhibitors, microtubule stabilizing agents with COX and LOX (5-lipoxygenase) inhibitors, dual binding site cholinesterase inhibitors with β-amyloid anti-aggregation properties, hybrid AChE and butyrylcholinesterase (BuChE) with anti-oxidant and neuroprotective properties, dual acting compounds targeting histaminergic system, hybrid AChE inhibitors with cannabinoid receptor antagonism, multifunctional chelators, hybrid BACE-1 inhibitors and metal chelators and dual acting γ-secreatse modulators with peroxisome proliferator activated receptor (PPAR)-γ.[5, 8-10]

Our study focuses on MTDLs acting on BACE-1 and inflammation concurrently. We have designed MTDLs comprising of two scaffolds in a single molecule to generate potential prototype ligand for complex AD treatment.

Design of molecules

BACE-1 is an aspartic protease enzyme developed as a one of the major targets for AD intervention. Based on the crystal structures of BACE-1 with ligands, catalytic machinery of the enzyme is well reported.[11] The aspartic dyad formed by Asp32 and Asp228 are located at the center of the binding site. BACE-1 catalyzes hydrolysis of peptide bonds by acid-base catalysis of water molecule present between aspartic acid dyad and forms tight hydrogen bond.[12] We aimed at identifying a potential moiety with ability to bind the enzymes catalytic aspartic dyad. Based on the reported literature we found, various thiadiazines are emerging as a BACE-1 inhibitor scaffold.[10,13-14] Iminothiadiazinane dioxide inhibitor was developed to exhibit selectivity of BACE-1 over BACE- 2 by forming H-bond with ASP32 and Asp228.[11] Verubecestat (MK-

8931-**1**) is a clinical candidate developed by Merck as a BACE-1 inhibitor contains iminothiadiazinane dioxide core scaffold with 2.2 nM K_i for BACE-1.[10,13] 5‑Aryl-1-imino-1-oxo-[1,2,4]thiadiazines (**2**) exhibited BACE-1 inhibition at IC_{50} of 0.009 nM.[15] (S)-3-amino-5-(3-chloro-4-(5-(prop-1-yn-1-yl)pyridin-3-yl)thiophen-2-yl)-2,5-dimethyl-5,6-dihydro-2*H*-1,2,4-thiadiazine 1,1-dioxide (**3**) showed BACE-1 inhibitory activity with the IC_{50} value of 2.4 nM.[14] These molecules signify the therapeutic importance of thiadiazines as BACE-1 inhibitors.

Neuronal inflammation is consider to be the downstream factor for the AD generation. The COX-1 and COX-2 expression are beneficial for neurodegeneration in AD. COX-1 is expressed in the glia and neurons of the AD brain. Little role of COX-1 is reported for the inflammatory mechanism through its glia expression. While the COX-2 expression is preferentially elevated in neurons with amyloid plaques and neurofibrillary tangles. Therefore, selective COX-2 inhibitors might influence the AD progression and non-selective COX-1 and COX-2 inhibitors mediate the anti-Alzheimer's effect by acting on glia and neurons. Thus, the design strategy for COX inhibitors with CNS penetration ability can be an effective solution for AD threat. Our lab has been exploring various small heterocycles as anti-inflammatory agents. Thiazole moiety has been established as a privileged structure to confer the drug likeliness properties. Also, the H-bond donor as well as H-bond acceptor features of thiazole are advantageous for H-bonding to the receptor, which impart the therapeutic activity.[16] Methyl 3-(4-(dimethylamino)-2-(methylamino)thiazol-5-yl)-2-(methoxyimino)-3-oxopropanoate (**4**) is reported as an anti-inflammatory agent with 83% inhibition of rat paw edema in acute inflammation and 66% inhibition of rat paw edema in chronic inflammation.[16] 2-(4-Chlorophenyl)-3-(4-methyl-2-(phenylamino)thiazol-5-yl)naphthalen-1(2*H*)-one (**5**) showed 72% inhibition of edema in acute

inflammation rat model.[17] Based on the reported literature, design of multitarget-directed ligands for BACE-1 enzyme and inflammation using thiadiazines and thiazoles is depicted in Figure 1.

INSERT FIGURE 1 HERE

Figure 1. Design strategy of MTDLs for AD

Results & Discussion:

Docking studies

To obtain substantial or rather conclusive theoretical evidence of therapeutic activity, the thiazolyl-thiadiazines were virtually screened by docking studies using Schrödinger software.[16] In the process, a library of thiazolyl-thiadiazines was prepared as shown in Figure 2 and docked against BACE-1, BACE-2, Cathepsin D, COX-1 and COX-2 enzymes. BACE-2 enzyme is a homolog of BACE-1 enzyme with nearly 64% of structural similarity and it can efficiently cleave APP but cannot form β-amyloid plaques. An important criterion to fulfill is selectivity of BACE-1enzyme over BACE-2 and Cathepsin D. Cathepsin D is a lysosomal aspartic endopeptidase associated with apoptosis regulation, metabolic degradation of intracellular proteins, stimulation and downgrading of polypeptide growth factors and hydrolysis of low-density lipoprotein (LDL). Non-inhibition of Cathepsin D is essential for the cell viability. Therefore, compounds with the best docking score values against BACE-1 and least docking scores against BACE-2 and Cathepsin D were selected for synthesis.

β-amyloid plaques and the damaged neurons induce inflammatory response as a natural phenomenon due to cell damage. The elevated levels of prostaglandins can be attributed to COX-1 and COX-2 enzymes. Also, certain pro-inflammatory substances are released from the activated microglia *viz.* reactive oxygen species (ROS), interlukin-1, interlukin-6 and tumor necrosis factor alleviate the AD progression. Thus, this increased oxidative stress causes the

neuronal cell degradation and amyloid-β neurotoxicity. To check the anti-inflammatory potential of designed molecules docking studies were performed using COX-1 and COX-2 enzymes. Noteworthy interactions between the molecules and catalytic pocket of BACE-1, COX-1 and COX-2 enzymes were observed during this scrutiny. Compounds with single target efficacy were forbidden from further studies as they deviate from our approach to target multiple enzymes. Results of top ranked compounds are displayed in Table 1 (For specific substitutions R^1, R^2 and R^3 refer Scheme 3 &4). Compounds showing least docking scores are mentioned in "Supporting Information".

INSERT FIGURE 2 HERE

Figure 2. General structure for docking library

$R^1 = R^2$ = H, Ph, 4-OCH_3-Ph, 4-CH_3-Ph, 4-F-Ph, 4-Cl-Ph, 3,4-di-Cl-Ph, 4-NO_2-Ph, 3,4-$(CH_3)_2$-Ph, 4-CF_3-Ph

R^3 = H, Ph, CH_3, $N(CH_3)_2$, CH_2-Ph

Table 1. Results of docking studies

Code	Docking Score				
	BACE-1	**BACE-2**	**Cathepsin D**	**COX-1**	**COX-2**
6a	-7.3	-4.5	-4.2	-8.1	-9.0
6b	-7.4	-4.3	-5.2	-8.5	-9.3
6c	-6.9	-4.6	-5.0	-8.7	-8.4
6d	-7.5	-4.1	-4.5	-9.2	-9.6
6e	-6.9	-4.4	-4.3	-8.9	-8.3

6f	-6.8	-4.0	-4.2	-8.0	-8.0
6g	-7.0	-4.3	-4.2	-8.0	-8.1
8a	-6.7	-4.0	-4.4	-8.4	-8.7
8b	-7.1	-4.4	-4.5	-8.4	-8.7
8c	-6.9	-4.5	-4.4	-8.3	-8.2
AZD3839	**-8.8**	-4.3	-4.4	-5.6	-5.5
Diclofenac	-3.6	-3.2	-3.5	**-8.7**	**-8.4**
Celecoxib	-4.9	-4.7	-4.5	-11.8	**-12.2**
Hydroxyethylenamine inhibitor	-5.2	**-11.8**	-4.6	-4.2	-5.0

Docking results were further extended as given in Figure 3A & 3B. The crystal structures of BACE-1 (PDB ID: 4B05) and COX-2 (PDB ID: 3LN1) enzymes were employed to conduct docking studies. Binding interactions and docking scores were considered for binding affinity of compounds with the respective enzymes. A side by side overlay of most potent compound **6d** with clinical candidate (AZD839) on BACE-1 enzyme binding site is demonstrated in Figure 3A. Figure 3B represents the overlay of standard drug Celecoxib and compound **6d** for COX-2 binding site influence. Binding interactions with the catalytic amino acid residues are found to be similar to that of reference drugs.

INSERT FIGURE 3A & 3B HERE

Figure 3. Docking study results **A)** Overlay of compound **6d** (green) with AZD3839 (orange) docked into the catalytic region of BACE-1. Compound **6d** showed H-bonding interactions (yellow dotted line) with aspartic acid dyad Asp32, Asp228 and π-π staking interaction (blue dotted line) with Tyr71. Docking score value was -7.5.

AZD3839 showed H-bonding interactions with Asp32, Asp228, Trp76 and π-π stacking interactions with Tyr71 and Phe108 with docking score of -8.8. **B)** Overlay of compound **6d** (green) with Celecoxib (orange) docked into COX-2 binding site. Compound **6d** showed H-bonding interaction with Tyr341, π-π stacking interactions with Tyr341, Trp373, Tyr371 and π-cation interaction (green dotted line) with Arg106. Docking score value was -9.6. Celecoxib showed H-bonding interactions with Tyr341, Ser339, Arg499, Phe504 and π-cation interaction with Arg106 with docking score of -12.2.

From the library of our designed molecules, those with the best docking scores against BACE-1 and inflammatory pathway enzymes were selected for synthesis. A complete synthetic route for compounds **6a-e & 8a-c** is portrayed in Scheme 1 to 4.

Prediction of physicochemical properties

An examination of physicochemical properties of central nervous system (CNS) targeting molecules is necessary from the view point of developing drug like molecules. Many active molecules fail to emerge out as drug candidates at the later stage of drug discovery due to lower blood brain barrier permeability. Hence, prediction of physicochemical properties of the molecules were carried out using Qikprop module of Schrödinger (Table 2)[18]. The selected compounds were found to obey the Lipinski's rule of five and Jorgensen's rule of three. Some other physicochemical parameters like QPlogBB, QPlogPo/w, QPPCaco, %HOA and QPlogHERG were also predicted. Compounds showed satisfactory drug likeliness properties with higher BBB permeation capacity and lower toxicity by HERG inhibition.

Table 2. Physicochemical properties prediction

Code	QPlogBB[a]	QPlogPo/w[b]	QPPCaco[c]	%HOA[d]	QPlogHERG[e]
6a	-0.11	6.40	3459	100	-6.43

6b	0.23	6.60	3452	100	-6.40
6c	-0.04	6.49	3414	100	-8.04
6d	0.24	6.51	3408	100	-7.70
6e	-0.01	6.31	3488	100	-6.40
6g	0.05	6.51	3410	100	-7.86
6f	0.21	6.46	3472	100	-7.95
8a	-0.54	3.89	857	100	-7.96
8b	-0.45	4.15	857	100	-7.83
8c	-0.40	4.40	855	100	-7.98
AZD3839	-0.629	4.35	500	100	-6.42
Diclofenac	-0.155	4.50	398	100	-2.95
Celecoxib	-0.780	3.34	358	92	-5.78

[a]QPlogBB: Predicted brain/blood partition coefficient (-3.0 to 1.2), [b]QPlogPo/w: Predicted octanol/water partition coefficient (-2.0 to 6.5), [c]QPPCaco: Predicted Caco-2 cell permeability (<25 poor, >500 great), [d]%HOA: Predicted human oral absorption (>80% is high, <25% is poor), [e]QPlogHERG: Predicted IC_{50} value for blockage of HERG K+ channels (below -5)

Chemistry

The designed compounds were synthesized as per the Schemes 1-4. Scheme1 demonstrates the synthesis of intermediates - substituted *N*-phenylhydrazinecarbothioamide **3a-e.** Reaction of substituted anilines in presence of TEA and carbon disulfide in THF at 0-5 °C yielded dithiocarbamate salt. This salt was further treated with TEA and ethyl chloroformate in chloroform at RT to get substituted isothiocyanatobenzenes **2a-f.** Synthesis of substituted *N*-

phenylhydrazinecarbothioamides **3a-e** were carried out using substituted isothiocyanatobenzenes in presence of hydrazine hydrate in THF at RT.

INSERT SCHEME 1 HERE

Scheme 1. Synthesis of substituted *N*-phenylhydrazinecarbothioamides

Reagents and Conditions: (a) TEA (3.2 eq), CS_2 (1.0 eq), 0-5 °C, THF, 6-7 hr; (b) TEA (1.0 eq), ethyl chloroformate (1.1 eq), 0 °C to RT, chloroform, 2 hr; (c) hydrazine hydrate, RT, THF, 2 hr

2-Chloro-1-(4-phenyl-2-(phenylamino)thiazol-5-yl)ethanone derivatives **5a-d** were synthesized as depicted in Scheme 2. Isothiocyanatobenzene reacted with *N*,*N*-diethylbenzimidamide in ethyl acetate at RT to yield *N*,*N*-diethyl-N'-(phenylcarbamothioyl)benzimidamide **4a-d.** Substituted 2-chloro-1-(4-phenyl-2-(phenylamino)thiazol-5-yl)ethanones were synthesized from **4a-d** using 1,3-Dichloropropan-2-one in acetonitrile at RT as described in Scheme 2.

INSERT SCHEME 2 HERE

Scheme 2. Synthesis of substituted 2-Chloro-1-(4-phenyl-2-(phenylamino)thiazol-5-yl)ethanones

Reagents and Conditions: (d) *N*,*N*-diethylbenzimidamide (1.0 eq), RT, ethyl acetate, 3-4 hr; (e) 1,3-Dichloropropan-2-one (1.5 eq), RT, acetonitrile, 3-4 hr

Scheme 3 depicts the reaction of final compounds **6a-g**. Reactions of the intermediates **3a-e** and **5a-d** were carried out by heating in THF at 70 °C for 6-7 hr to afford substituted *N*-phenyl-5-(4-phenyl-2-(phenylamino)thiazol-5-yl)-6*H*-1,3,4-thiadiazin-2-amines (final compounds).

INSERT SCHEME 3 HERE

Scheme 3. Synthesis of substituted *N*-phenyl-5-(4-phenyl-2-(phenylamino)thiazol-5-yl)-6*H*-1,3,4-thiadiazin-2-amines (Final compounds)

Reagents and Conditions: (f) 70 °C, THF, 6-7 hr

Final compounds **8a-c** were synthesized as per the Scheme 4. Hydrazinecarbothioamide was reacted with intermediate **5b-d** in THF at 70 °C for 6-7 hr to get the final compounds substituted 5-(4-phenyl-2-(p-tolylamino)thiazol-5-yl)-6*H*-1,3,4-thiadiazin-2-amine **8a-c.**

INSERT SCHEME 4 HERE

Scheme 4. Synthesis of substituted 5-(4-phenyl-2-(p-tolylamino)thiazol-5-yl)-6*H*-1,3,4-thiadiazin-2-amines (Final compounds)

Reagents and Conditions: (f) 70 °C, THF, 6-7 hr

Biological Evaluation

In vitro BACE-1 inhibition assay

The molecules (**6a-g and 8a-c**) were investigated by *in vitro* BACE-1 inhibition assay (Table 3). IC_{50} values were obtained and compared with the reference molecule AZD3839.[20] Compounds **6a-g** have aromatic-NH substitutions and **8a-c** have NH_2 substitutions at 2^{nd} position of thiadiazine. Compounds bearing trifluromethyl substitution at R^1 position were found to be the most active BACE-1 inhibitors. Compounds **6b** and **6d** showed BACE-1 inhibition with IC_{50} of 9 μM. As shown in Figure 3A, **6d** had binding interactions with the catalytic aspartic dyad of the enzyme Asp32 and Asp228 along with π-π staking interaction with Tyr71. Docking score value of **6b** and **6d** were found as -7.4 & -7.5, respectively. Compounds **6b** and **6d** have similarity in structure except the R^2 position with methyl group in **6b**. Compound **6a** has methoxy group at R^1 position which showed BACE-1 inhibition with IC_{50} of 11 μM. NH_2 group at 2^{nd} position of thiadiazine moderately inhibited BACE-1 with IC_{50} of 50, 29 and 20 μM in compound **8a**, **8b** and **8c**, respectively. Fluoro and chloro substitutions at R^2 position favored BACE-1 inhibitory

activity in **8b** and **8c**. Compounds **6f** and **8a** showed BACE-1 enzyme inhibition with IC_{50} of 50 µM. Whereas, **6e** and **6g** were found to be less potent with IC_{50} greater than 100 µM.

Table 3. *In vitro* inhibitory potencies (IC_{50}) of compounds against BACE-1 and *in vivo* % edema inhibition against acute inflammation rat model

Compound	**BACE-1 [IC_{50} (µM) ± SEM[a]]**	**% inhibition of edema against acute inflammation[b] [Mean ± SEM]**
6a	11 ± 0.08	48 ± 0.45
6b	9 ± 0.35	63 ± 0.6
6c	40 ± 0.2	48 ± 0.75
6d	9 ± 0.09	70 ± 0.4
6e	112 ± 0.08	56 ± 0.5
6f	50 ± 0.09	70 ± 0.55
6g	114 ± 0.5	29 ± 0.9
8a	50 ± 0.09	67 ± 0.7
8b	29 ± 0.7	60 ± 1.0
8c	20 ± 0.5	29 ± 0.95
Diclofenac	NT	72 ± 0.65

[a]IC_{50} values are reported as concentration of each compound resulting in 50% inhibition. Data represented as Mean ± SEM (n=3)

[b]Data shown are refer to the % change in edema size relative to the disease control group. Statistical analysis was performed by One-way ANOVA followed by Tukey's multiple comparison test. Mean ± SEM (n=6 animals/group) *$p<0.05$

NT Not Tested

In vivo carrageenan induced acute inflammation study

Another crucial aspect in understanding the efficacy of these developed molecules against AD was estimated by carrying out *in vivo* acute inflammation study in rats.[21] We observed satisfactory results for compounds (**6a-g and 8a-c**), as compared with reference drug; Diclofenac sodium. % edema inhibition in case of compounds **6d**, **6f** and **8c** was found to be 70%, 70% and 67 %, respectively. In case of Diclofenac, 72 % inhibition was noticed, as mentioned in Table 4. Compounds **6b**, **6e**, **8a** and **8b** showed anti-inflammatory activity with 63%, 56%, 67% and 60% of rat paw edema. Importantly, these developed molecules fit into the catalytic pocket of COX-1 and COX-2 enzyme non-selectively and subsequently elicit anti-inflammatory activity as evidenced from the present study.

In vivo formalin induced chronic inflammation study

As illustrated above, compounds **6b**, **6d** and **6f** were found as promising agents with BACE-1 inhibition and acute anti-inflammatory properties. In spite of this, the results obtained were rather insufficient to identify these MTDLs as candidate for treatment of AD because chronic inflammation has been characterized to cause major AD mechanism reinforced by release of cytokines and chemokines from activated microglia and astrocytes.[22] Therefore, the developed MTDLs were further evaluated against the chronic inflammation model developed in rats.[21] It was very captivating to note that the % edema inhibition for compounds **6b**, **6d**, **6f** were 49%, 58% and 47%, respectively on the 5th day of chronic model. Celecoxib was taken as a reference drug and showed 68% edema inhibition on the 5th day as shown in Table 4.

Table 4. % edema inhibition against chronic inflammation rat model

Compound	% inhibition of edema in chronic inflammation [a][Mean ± SEM]

	Day 1	Day 2	Day 3	Day 4	Day 5
6b	45 ± 0.7	52 ± 1.1	53 ± 2.1	54 ± 1.4	49 ± 1.6
6d	54 ± 1.7	55 ± 0.4	59 ± 1.0	60 ± 2.0	58 ± 0.6
6f	49 ± 1.5	43 ± 1.2	39 ± 1.3	43 ± 0.9	47 ± 0.8
Celecoxib	67 ± 0.9	74 ± 0.6	70 ± 2.2	70 ± 1.5	68 ± 0.5

[a]Data shown are refer to the % change in edema size relative to the disease control group. Statistical analysis was performed by One-way ANOVA followed by Tukey's multiple comparison test. Mean ± SEM (n=6 animals/group) *$p<0.05$

$AlCl_3$ induced Alzheimer's disease model

Taking into account the potency of compound **6d** against BACE-1, acute and chronic inflammation, it was further examined for its effect on $AlCl_3$ induced rat model of AD.[23] During the course of this examination the behavioral parameters were assessed by using pole climbing apparatus[24], elevated plus maze[25] and Y-maze.[26] We wanted to ascertain the memory enhancing effects of compound **6d** in the developed model of AD. In this purview, elevated plus maze test (EPM) was used for testing the spatial working memory of compound **6d** treated rats. Transfer latency (TL) i.e. the time taken by an animal to move from an open arm to enclosed arm was calculated. It was measured as a parameter of animal's ability to recall the location of enclosed arms since animals feel unsafe in open and high spaced maze. Interestingly, rats treated with compound **6d** showed significant improvement from the $AlCl_3$ induced memory impairment and significantly decreased TL as shown in Figure 4A. Further, based on the rodent's innate tendency to explore new environment, Y-maze test was carried out to test immediate working memory of **6d** treated rats. In this test, they showed preference towards novel unexplored arm over the previously explored one. Also, % alteration was measured and animals treated with compound **6d** showed elevation in the % alteration which indicated an increase in their cognitive function as

shown in Figure 4B. Consequently, compound **6d** when tested in the rat model of conditioned avoidance response (CAR), it was found to reverse the amnesic effect of $AlCl_3$, in comparison to the disease group as displayed in Figure 4C, Compound **6d** decreased the CAR and showed effective measure of cognition compared to $AlCl_3$ treated animals.

INSERT FIGURE 4A, 4B, 4C AND FIGURE 4 DATA LABEL HERE

Figure 4. Effect of compound **6d** on behavioral parameters of AD. NC= Normal control group animals treated with normal saline, DC = Disease control group animals treated with $AlCl_3$ (4.2 mg/kg *i.p.),* PC = Positive control group animals treated with $AlCl_3$ (4.2 mg/kg *i.p*) and Meloxicam (5.0 mg/kg, *per oral*), 6d = MTDL group animals treated with $AlCl_3$ (4.2 mg/kg *i.p*) and compound **6d** (50.0 mg/kg, *per oral*) **A)** transfer latency (Sec) was calculated using EPM test. Data expressed as mean TL (Sec) ± SEM. **B)** % alteration assessed by Y-maze apparatus expressed as mean % alteration ± SEM. **C)** inhibition of CAR by compound **6d** on $AlCl_3$ induced amnesia using pole climbing apparatus. Results represent the mean of CAR (Sec) ± SEM. Asterisk denotes statistical significance ($^{*}p<0.05$) when compared to NC and ($^{\#}p<0.05$) when compared to DC, using two-way ANOVA followed by Tukey's multiple comparison test.

Oxidative stress is an important marker of AD.[27] We studied the free radical scavenging effect of compound **6d** on $AlCl_3$ treated animals. Anti-oxidative benefits of compound **6d** were observed in the rat brain homogenates when tested by lipid peroxidation (LPO) levels and superoxide dismutase (SOD) activity. High level of malonaldehyde (MDA), a marker for LPO indicates higher oxidative stress.[28,29] $AlCl_3$ treated rats showed significant elevation in MDA levels and interestingly, MDA level was noticed to have significantly reduced in animals treated with compound **6d** ($^{\#}p<0.05$) in comparison to DC group (Figure 5A). Additionally, as expected the anti-oxidant enzyme SOD activity was significantly decreased in AD induced animals.[28] Notably, SOD activity was found to be significantly increased in compound **6d** treated animals as compared to the animals in the DC group ($^{\#}p<0.05$) as shown in Figure 5B. These results signify the anti-oxidative properties of compound **6d**.

INSERT FIGURE 5A & 5B HERE

Figure 5. Anti-oxidative effect of compound **6d**: **A)** Lipid peroxidation (LPO) expressed as MDA level in rat brain homogenates **B)** Super oxide dismutase (SOD) activity in rat brain homogenates. Data shown as Mean ± SEM (n=6 animals/group) *p<0.05 when compared to NC and $^{\#}$p<0.05 when compared to DC group using one-way ANOVA followed by Tukey's multiple comparison test.

Haematological parameters estimation:

Haemoglobin and haematocrit level were estimated for all the groups of animals. Results indicated that there was a significant decrease in the haemoglobin (HGB) and haematocrit (HCT) level in PC group animals treated with 5 mg/kg of Meloxicam. Whereas, DC and compound **6d** treated animals showed HGB and HCT level same as that of NC animals (Figure 6A & 6B). These studies indicated that Meloxicam causes loss of blood due to the gastric injury. Which was further confirmed by results of gastro-intestinal (GI) safety studies.

INSERT FIGURE 6A & 6B HERE

Figure 6. Estimation of haematological parameters: **A**) Estimation of HGB level in all the groups. PC animals showed significant decrease in the HGB level compared to all the groups. Here, data presented as Mean ± SEM (*p<0.05). **B**) HCT level estimation in all the groups indicated that there was a significant decrease in the HCT level in PC group when compared to all the groups. Data expressed as Mean ± SEM (*p<0.05) by using one-way ANOVA followed by Tukey's multiple comparison test.

Estimation of Serum biochemical parameters:

From the study of serum biochemical parameters, it was observed that there was no significant difference in all the groups' serum albumin level (Figure 7A). Whereas, PC and DC animals showed significant difference in the total protein when compared with NC and compound **6d** treated animals (Figure 7B).

INSERT FIGURE 7A & 7B HERE

Figure 7: Serum albumin & Total protein estimation: **A**) Graph represent estimation of serum albumin level in all the groups. There was no significant difference in the serum albumin level in all the groups. **B**) Total protein level was significantly different in DC and PC group. Decrease in the total protein level was observed in DC and PC group when compared to NC and compound **6d** treated animals. Data expressed as Mean ± SEM (*$p<0.05$) by using one-way ANOVA followed by Tukey's multiple comparison test.

$AlCl_3$ by causing oxidative damage to the neuronal cells[30] forms aggregates of amyloid peptides which leads to the degeneration of neuronal cells.[31] To observe the effect of compound **6d** on cellular morphology of hippocampal neuronal cells, histopathological studies by hematoxylin-eosin (HE) stain was employed. Results of HE stain in rat brain indicated the curative effect of compound **6d** against the neuronal degeneration. Figure 8A represents the normal and intact hippocampal neurons (NC rats). In Figure 8B, it can be observed that neurons of DC animals have degenerated. While, in PC group (Figure 8C) and compound 6d treated group (Figure 8D) healthy and intact hippocampus neuronal region similar to that of NC animals was observed. These results proved that in compound **6d** treated animals, there was no sign of neuronal cell degeneration as compound **6d** protected the neurons from the detrimental effect of $AlCl_3$. Eventually it signifies the protective effect of compound **6d** against oxidative-stress and amyloid plaques aggregations induced cell damage. In addition to this, the effect of compound **6d** on amyloid plaques formation was checked by Congo red staining and compound **6d** was found to act as an excellent anti-amyloid agent (Figure 9). The serial sections were stained with Congo red to detect the amyloid plaques in the cortex region of the brain. Animals treated with $AlCl_3$ showed formation of amyloid plaques in the cortex region of the brain. Whereas, compound **6d** treated group did not show plaques in the cortex region of the brain.

INSERT FIGURE 8 HERE

Figure 8. Typical microscopic HE stained sections (under 100X magnification) of brain in all the groups. **A**) NC rat brain showed healthy and intact neurons **B**) DC rat brain showed neuronal loss with shrunken and degenerated hippocampal region **C**) PC rat brain showed intact neurons but thin hippocampal region and **D**) Compound **6d** treated rat brain showed intact, healthy neurons with dense hippocampal region

INSERT FIGURE 9 HERE

Figure 9: Typical microscopic Congo red sections (under 100X magnification) of brain in all the groups: A) NC rat brain without any amyloid plaques B) DC rat brain with amyloid plaques in the cortex region C) PC rat brain showed no amyloid plaque region in the cortex D) compound **6d** treated rat brain had no plaque in the cortex.

Gastro-intestinal (GI) safety studies of compound 6d

Macroscopic evaluation: PC animals treated with Meloxicam showed gastric and intestinal damage. Lesion indices of PC treated animals in stomach and intestine were found to be 12.19 ± 0.7 mm and 29.15 ± 1.3 mm, respectively. Whereas, compound **6d** treated rats did not show any haemorrhagic damage in the stomach and intestine as shown in Figure 10.

INSERT FIGURE 10 HERE

Figure 10: Lesion index. Data expressed as Mean ± SEM (*$p<0.05$) by using two-way ANOVA followed by Tukey's multiple comparison test.

Histopathological studies of stomach and intestine: Microscopic evaluation of stomach and intestinal HE stained sections revealed focal erosions and perforations in the stomach of PC rats. Moreover, epithelium erosions and stratifications were observed in intestines of PC treated animals. Whereas, DC group and compound **6d** treated animals did not show any focal erosions and damage in the stomach and intestinal region as shown in Figure 11 & 12. These studies proved the gastric safety of compound **6d** when compared to the standard drug Meloxicam.

INSERT FIGURE 11 HERE

Figure 11: Typical microscopic HE stained sections (under 100X magnification) of stomach in all the groups. **A**) NC group without any gastric damage **B**) DC rats did not show erosions **C**) PC treated rats showed focal erosions and perforations indicated by an arrow **D**) Compound **6d** treated animals had no erosions or perforations in stomach

INSERT FIGURE 12 HERE

Figure 12: Typical microscopic HE stained sections (under 100X magnification) of intestine in all the groups. **A**) NC rats without epithelium damage **B**) DC rats did not show any erosions **C**) PC rats showed epithelium erosions and stratification indicated by an arrow **D**) Compound **6d** treated animals with intact intestinal epithelium

Although, Meloxicam is a potent non-steroidal anti-inflammatory drug (NSAIDs) being used in AD, it is not gastrointestinal (GI) safe. NSAIDs-induced gastroenteropathy is a serious risk against the usage of such NSAIDs. It is essential to note that, in present study, while GI adverse events were observed in all the NSAIDs (Diclofenac, Celecoxib and Meloxicam)[32-34], compound **6d** despite having proportional anti-inflammatory activity demonstrated excellent GI safety in comparison to standard drug Meloxicam.

Conclusion

AD has become a major burden worldwide and it is the 6th leading cause of death in US population. The currently available drugs do not possess disease modifying potential, which is the major drawback for AD treatment. Even though drugs targeting β-amyloid plaques have recently emerged to be a useful tactic to get the disease modifying benefits, the reported anti-amyloid moieties have failed during clinical trials. Hence, to target the multi-factorial nature of AD, and to overcome the drawbacks of single targeted drugs; multitarget drug design approach seems to be an appropriate strategy in quest for new anti-Alzheimer's agents. Inflammation is another major hallmark for AD pathogenesis. Anti-inflammatory activity may hold the greater potential in AD treatment by reducing the oxidative damage and plaque formation. Thus to achieve the disease modifying benefits, BACE-1 inhibitory and anti-inflammatory activities are

conjoined in one single molecule. We designed thiazolyl-thiadiazines as MTDLs for the first time, acting on BACE-1 and inflammation simultaneously. *In silico* docking studies suggested the multitargeted profile of these molecules. They were found to interact with enzyme's catalytic domain of BACE-1, COX-1 and COX-2. These MTDLs showed effective results in *in vitro* BACE-1 inhibition assay and *in vivo* acute and chronic anti-inflammatory studies. One of the molecules; compound **6d** showed promising result in behavioral studies conducted in rats. Compound **6d** was found to have excellent anti-oxidant properties. It was demonstrated to have anti-amyloid potency and neuroprotective effect which is an advantageous feature of these studies. The results are encouraging and may lead to the development of disease modifying treatment for AD. Furthermore, the GI safety profile of the molecule offers excellent advantage in relation to the oral toxicity over NSAIDs.

Our future endeavor is to bring this multifaceted category of molecules to the forefront of therapeutic agents for the management of AD and many other diseases as well and emerge as a forerunner in this field. Translation of this knowledge is eagerly awaited.

Materials & methods

Reagents and solvents were purchased from commercial suppliers and were used without further purification. Melting points were determined using scientific melting point apparatus (Veego; Model VMP-DS) and are uncorrected. FT-IR spectra were obtained using IR Affinity 1 by Shimadzu. Mass spectra were recorded using LC-ESI-MS (Perkin Elmer mass spectrometer). HRMS spectral analysis was done by waters Q-TOF micromass (ESI-MS). ^{1}H NMR and ^{13}C NMR samples analysis were carried out using Bruker Avance II 400 MHz NMR spectrophotometer with chemical shift values represented in parts per million. Signals are described as s (singlet), d (doublet), t (triplet), q (quartet), m (multiplet) and dd (doublet of

doublets). Reaction monitoring was done by thin layer chromatography (TLC, Merck, Pre-coated). TLC spot visualization was done under UV light using UV chamber. Purity of compounds was determined by using SHIMADZU-LC-2010 HPLC. Schrödinger software was used for *in silico* docking and physical properties prediction. Fluorimetric BACE-1 inhibition assay readings were taken from Varioskan® Flash multimode plate reader. Paw volumes were recorded using manual mercury plethysmometer. Polytron homogenizer (Kinematica, Switzerland) was used for homogenization. Centrifugation was carried out using Sorvall Legend X1R centrifuge (Thermo Scientific). Samples were vortexed in Vortex Mixer (Eltek, VM301). UV-Visible absorbance of the samples were taken using UV/Visible Spectrophotometer Shimadzu UV-1800. Serum albumin and total protein were determined using fully automated random access clinical chemistry analyser Transasia EM 360. Haemoglobin and haematocrit level estimation were obtained using VetScan HM-5. Histopathological slides were observed under optical microscope ProgRes C3 OLYMPUS, U-TV1 X, Japan.

Experimental procedures

1) Docking studies

Docking studies were carried out using Maestro 11.1.012 software of Schrödinger, LLC, New York, NY, 2017, USA.[18]

Ligand preparation: Library of molecules was generated and all the structures were drawn and cleaned up in the Maestro software 2D sketcher. Ligprep module was used for the energy minimization of all the structures using OPLS3 force field and possible states were obtained by using Epik (pH 7.0). Results of the Ligprep studies were taken further for docking process. The general structure for library of thiazolyl-thiadiazines is given in Figure S1. Different R^1 and R^2 substituents were taken for docking process.

Protein preparation

BACE-1 protein preparation: Docking studies were performed using BACE-1 crystal structure from protein data bank. PDB ID: 4B05 was retrieved from protein data bank which contains complex structure of BACE-1 with the bound ligand AZD3839 (clinical candidate).[20] Protein structure was prepared using protein preparation wizard of Schrödinger 11.1.012 software. Bond orders were assigned and hydrogens were added to the structure. Zero order bonds to metals and disulfide bonds were added. Missing side chains were added using prime and water molecules within 5 Å of het groups were removed. All the ions were deleted and protein structures were optimized using OPLS3 force field and minimized for receptor grid generation. Grid was obtained at the centroid of the ligand (AZD3839) of BACE-1 receptor.

BACE-2 protein preparation: Crystal structure of human BACE-2 in complex with a hydroxyethylenamine transition-state inhibitor was retrieved from the protein data bank (PDB ID: 2EWY).[35] Protein preparation was carried out using the same protocol as described in BACE-1 protein preparation. Chain A was used for the docking study.

Cathepsin D protein preparation: Crystal structure of Cathepsin D (PDB ID: 1LYW) was retrieved from protein data bank.[36] Protein was prepared using protein preparation wizard by adding bond orders, hydrogens and removing water within 5 Å of het groups. Protein structure was optimized and minimized. Binding site generation was carried out by using SiteMap module of Schrödinger.[37] Top ranked potential binding sites were identified by using SiteScore. Highest ranked binding site was selected for receptor grid generation. Grid was generated at the binding site pocket of the enzyme and used for the docking process.

COX-1 protein preparation: Crystal structure of COX-1 in complex with Celecoxib (PDB ID: 3KK6)[38] was used for the docking process. All the steps for the protein preparation were followed as described in BACE-1 protein preparation protocol.

COX-2 protein preparation: Structure of COX-2 with co-crystallized Celecoxib ligand (PDB ID: 3LN1) was used for the docking process.[39] All the steps for the COX-2 protein preparation were followed as per the given protocol of BACE-1 protein preparation using chain A of the enzyme.

Docking study: Ligand docking was performed using Glide module of Schrödinger suite. Extra precision (XP) mode was used for the docking of all the molecules with proteins. Docking score and interactions of ligands with protein were taken into consideration for predicting activity of the molecules. Validation of docking process was done by re docking of co-crystallized ligand with the proteins.

2) Physicochemical properties prediction

Prediction of physicochemical properties of the compounds was done using QikProp application of Schrödinger.[40] Properties like brain/blood partition coefficient (QPlogBB), octanol/water partition coefficient (QPlogPo/w), Caco-2 cell permeability (QPPCaco), % human oral absorption (HOA), HERG inhibition (QPlogHERG) were taken into consideration for the brain permeability and toxicity prediction of the molecules.

3) Chemistry

General procedure A: Synthesis of substituted hydrazinecarbothioamides (3a-e)

To the solution of substituted amines **1a-e** (1.0 eq) in THF, addition of triethylamine (3.2 eq) and carbon disulfide was done at 0-5 °C. Reaction was allowed to stir for 6-7 hr. Formation of dithiocarbamate salt was confirmed by TLC (Methanol: Hexane: Ethyl acetate =

0.5:3:1.5). It was filtered off and dried. Salt was dissolved in chloroform and addition of triethylamine (1.0 eq) and ethyl chloroformate (1.1 eq) was done at 0-5 °C and continued to stir at room temperature (RT) for 2 hr. Reaction was monitored by TLC (Hexane: Ethyl acetate = 1:4). After completion of reaction, 3M HCl was added to the reaction mixture. Chloroform layer was separated and washed with water (3×50 ml). Chloroform was evaporated under *vacuo* and dried over sodium sulfate to yield **2a-e**. Purification of **2a-e** was done by column chromatography using 100% hexane as a mobile phase.

After that, **2a-e** (1.0 eq) was reacted with hydrazine hydrate in THF at RT for 2 hr. Reaction was monitored by TLC (Hexane: Ethyl acetate = 3:2). THF was evaporated under *vacuo* and crystallized using methanol to get pure white product of **3a-e**.

***N*-(4-methoxyphenyl)hydrazinecarbothioamide (3a)**

Synthesis of intermediate **2a** was done using starting material 4-methoxyaniline **1a**. **3a** was synthesized using 1-isothiocyanato-4-methoxybenzene **2a** and hydrazine hydrate as described in general procedure A. Colorless solid; Yield: 81%; Melting point: 162-164 °C; R_f: 0.30 (Hexane: Ethyl acetate = 3:2); LC-ESI-MS (m/z): 198.1 $[M+H]^+$

***N*-(4-(trifluoromethyl)phenyl)hydrazinecarbothioamide (3b)**

Synthesis of intermediate **2b** was done using starting material 4-(trifluoromethyl)aniline **1b**. **3b** was synthesized using 1-isothiocyanato-4-(trifluoromethyl)benzene **2b** and hydrazine hydrate as described in general procedure A. Colorless solid; Yield: 83%; Melting point: 159-161 °C; R_f: 0.32 (Hexane: Ethyl acetate = 3:2); LC-ESI-MS (m/z): 236.0 $[M+H]^+$

***N*-(p-tolyl)hydrazinecarbothioamide (3c)**

Synthesis of intermediate **2c** was done using starting material p-toluidine **1c**. **3c** was synthesized using 1-isothiocyanato-4-methylbenzene **2c** and hydrazine hydrate as described in general procedure A. Colorless solid; Yield: 79%; Melting point: 165-167 °C; R_f: 0.28 (Hexane: Ethyl acetate = 3:2); LC-ESI-MS (m/z): 182.2 $[M+H]^+$

***N*-phenylhydrazinecarbothioamide (3d)**

Synthesis of intermediate **2d** was done using starting material aniline **1d**. **3d** was synthesized using isothiocyanatobenzene **2d** and hydrazine hydrate as described in general procedure A. Colorless solid; Yield: 72%; Melting point: 173-175 °C; R_f: 0.26 (Hexane: Ethyl acetate = 3:2); LC-ESI-MS (m/z): 168.2 $[M+H]^+$

***N*-(4-fluorophenyl)hydrazinecarbothioamide (3e)**

Synthesis of intermediate **2e** was done using starting material 4-fluoroaniline **1e**. **3e** was synthesized using 1-fluoro-4-isothiocyanatobenzene **2e** and hydrazine hydrate as described in general procedure A. Colorless solid; Yield: 71%; Melting point: 184-186 °C; R_f: 0.31 (Hexane: Ethyl acetate = 3:2); LC-ESI-MS (m/z): 186.2 $[M+H]^+$

General procedure B: Synthesis of substituted 1-(2-amino-4-phenylthiazol-5-yl)-2-chloroethanones (5a-d)

To a solution of *N,N*-diethylbenzimidamide[41] (1.0 eq) in ethyl acetate, isothiocyanatobenzene (1.0 eq) **2c-e** was added and stirred at RT for 3-4 hr. Progress of reaction was monitored by TLC (Hexane: Ethyl acetate = 7:3). Yellowish solid was filtered off, washed with hexane and dried to yield pure substituted *N,N*-diethyl-*N*'-(phenylcarbamothioyl)benzimidamide **4a-d**. After that, 1,3-Dichloropropan-2-one (1.5 eq) in acetonitrile was taken into round bottom flask and **4a-d** (1.0 eq) was added slowly. Reaction was allowed to stir for 3-4 hr at RT.

Progress of reaction was checked by TLC. (Hexane: Ethyl acetate = 7:3) and upon completion of reaction, reaction mixture was poured into ice cold water to get yellow precipitates of **5a-d**. Pure **5a-d** were obtained by crystallization using methanol.

2-Chloro-1-(4-phenyl-2-(p-tolylamino)thiazol-5-yl)ethanone (5a)

Intermediate **4a** was synthesized using starting material 1-Isothiocyanato-4-methylbenzene **2c**. Synthesis of **5a** was done using *N*,*N*-diethyl-*N*′-(p-tolylcarbamothioyl)benzimidamide **4a** and 1,3-Dichloropropan-2-one as described in general procedure B. Brown solid; Yield: 69%; Melting point: 171-173 °C; R_f: 0.50 (Hexane: Ethyl acetate = 3:2); LC-ESI-MS (m/z): 342.5 $[M]^+$, 344.5 $[M+2]^+$

2-Chloro-1-(4-phenyl-2-(phenylamino)thiazol-5-yl)ethanone (5b)

Intermediate **4b** was synthesized using starting material isothiocyanatobenzene **2d**. Synthesis of **5b** was done using *N,N*-diethyl-*N*′-(phenylcarbamothioyl)benzimidamide **4b** and 1,3-Dichloropropan-2-one as described in general procedure B. Brown solid; Yield: 75%; Melting point: 167-169 °C; R_f: 0.48 (Hexane: Ethyl acetate = 3:2); LC-ESI-MS (m/z): 328.5 $[M]^+$, 330.5 $[M+2]^+$

2-Chloro-1-(2-((4-fluorophenyl)amino)-4-phenylthiazol-5-yl)ethanone (5c)

Intermediate **4c** was synthesized using starting material 1-Fluoro-4-isothiocyanatobenzene **2e**. Synthesis of **5c** was done using *N,N*-diethyl-*N*′-((4-fluorophenyl)carbamothioyl)benzimidamide **4c** and 1,3-Dichloropropan-2-one as described in general procedure B. Brown solid; Yield: 75%; Melting point: 177-179 °C; R_f: 0.52 (Hexane: Ethyl acetate = 3:2); LC-ESI-MS (m/z): 346.5 $[M]^+$, 348.5 $[M+2]^+$

2-Chloro-1-(2-((4-chlorophenyl)amino)-4-phenylthiazol-5-yl)ethanone (5d)

Intermediate **4d** was synthesized using starting material 1-Chloro-4-isothiocyanatobenzene **2f**. Synthesis of **5d** was done using *N′*-((4-chlorophenyl)carbamothioyl)-*N,N*-diethylbenzimidamide **4d** and 1,3-Dichloropropan-2-one as described in general procedure B. Brown solid; Yield: 65%; Melting point: 183-185 °C; R_f: 0.53 (Hexane: Ethyl acetate = 3:2); LC-ESI-MS (m/z): 346.5 $[M]^+$, 348.5 $[M+2]^+$, 350.5 $[M+4]^+$

General procedure C for final compounds: Synthesis of substituted 5-(2-amino-4-phenylthiazol-5-yl)-6*H*-1,3,4-thiadiazin-2-amines (6a-g & 8a-c)

To a solution of substituted hydrazinecarbothioamides **3a-e** and hydrazinecarbothioamide **7a** (1.2 eq) in THF, addition of substituted 1-(2-amino-4-phenylthiazol-5-yl)-2-chloroethanones **5a-d** (1.0 eq) was done. Reaction mixture was allowed to stir for 6-7 hr at 70 °C. Reaction was monitored by TLC (Hexane: Ethyl acetate = 7:3). Reaction mixture was poured into cold water to get precipitates of **6a-g & 8a-c**. Compounds were purified by column chromatography to yield pure compounds. HPLC purity was determined using SHIMADZU-LC-2010 [Mobile phase (10 mM): KH_2PO_4 buffer: Acetonitrile (50:50); Column: Reverse phase; pH: 7]

***N*-(4-methoxyphenyl)-5-(4-phenyl-2-(p-tolylamino)thiazol-5-yl)-6*H*-1,3,4-thiadiazin-2-amine (6a)**

Final compound **6a** was synthesized using starting material *N*-(4-methoxyphenyl)hydrazinecarbothioamide **3a** and 2-Chloro-1-(4-phenyl-2-(p-tolylamino)thiazol-5-yl)ethanone **5a** as described in general procedure C. Pale yellow solid; Yield: 81%; Purity: 99.8%; Melting point: 177-179 °C; Molecular formula: $C_{26}H_{23}N_5OS_2$; LC-ESI-MS (m/z): 486.1 $[M+H]^+$; HRMS (TOF) *m/z* calcd for $C_{26}H_{23}N_5OS_2$ $[M+H]^+$

486.1344, found: 486.1142; IR (KBr, cm^{-1}): 3319.49, 2908.65, 1608.63, 769.60; ^{1}H NMR (400MHz, DMSO-d_6) δ: 2.254 (s, 3H, CH_3), 3.224 (s, 2H, CH_2), 3.718 (s, 3H, CH_3O), 6.865 (d, *J* = 8.8 Hz, 2H, meta to CH_3O), 7.131 (d, *J* = 8.4 Hz, 2H, ortho to CH_3O), 7.447-7.495 (m, 4H, CH_3-C_6H_4), 7.532 (d, *J* = 8.8 Hz, 2H, C_6H_5), 7.568-7.591 (m, 3H, C_6H_5), 10.439 (s, D_2O exchangeable, 1H, NH linked to thiazole), 10.452 (s, D_2O exchangeable, 1H, NH linked to thiadiazine); ^{13}C NMR (400 MHz, DMSO-d_6) δ: 20.42 (CH_3), 29.56 (CH_2), 52.51 (CH_3), 116.40 (2×CH, CH_3O-C_6H_4), 117.47 (2×CH, CH_3O-C_6H_4), 118.35 (2×CH, CH_3-C_6H_4), 122.03 (2×CH, C_6H_5), 124.78 (2×CH, CH_3-C_6H_4), 128.12 (CH, C_6H_5), 128.50 (CH, CH_3-C_6H_4), 128.96 (CH, CH_3-C_6H_4), 129.24 (C, C_6H_5), 129.56 (C, CH_3O-C_6H_4), 129.87 (C, thiazole), 134.81 (C, C_6H_5), 140.11 (C, CH_3O-C_6H_4), 141.36 (C, CH_3O-C_6H_4), 151.93 (C, thiazole), 157.45 (C, thiadiazine), 160.82 (C, thiazole), 170.71 (C, thiadiazine)

5-(4-Phenyl-2-(p-tolylamino)thiazol-5-yl)-*N*-(4-(trifluoromethyl)phenyl)-6*H*-1,3,4-thiadiazin-2-amine (6b)

Final compound **6b** was synthesized using starting material *N*-(4-(trifluoromethyl)phenyl)hydrazinecarbothioamide **3b** and 2-Chloro-1-(4-phenyl-2-(p-tolylamino)thiazol-5-yl)ethanone **5a** as described in general procedure C. Pale yellow solid; Yield: 64%; Purity: 99.9%; Melting point: 165-167 °C; Molecular formula: $C_{26}H_{20}F_3N_5S_2$; LC-ESI-MS (m/z): 524.1 $[M+H]^+$; HRMS (TOF) *m/z* calcd for $C_{26}H_{20}F_3N_5S_2$ $[M+H]^+$ 524.1112, found: 524.1035; IR (KBr, cm^{-1}): 3159.40, 2916.37, 1508.33, 769.60; ^{1}H NMR (400MHz, DMSO-d_6) δ: 2.259 (s, 3H, CH_3), 3.274 (s, 2H, CH_2), 7.148 (d, *J* = 8.4 Hz, 2H, meta to CF_3), 7.469-7.479 (m, 3H, CH_3-C_6H_4 & C_6H_5), 7.538 (d, *J* = 8.4 Hz, 2H, ortho to CH_3), 7.583-7.593 (m, 2H, CF_3), 7.643 (d, *J* = 8.4 Hz, 4H, C_6H_5), 9.789 (s, D_2O exchangeable, 1H, NH linked to thiazole), 10.488 (s, D_2O exchangeable, 1H, NH linked to

thiadiazine); ^{13}C NMR (400 MHz, DMSO-d_6) δ: 20.26 (CH_3), 25.36 (CH_2), 116.72 (2×CH, CF_3-C_6H_4), 117.76 (CH, CH_3-C_6H_4), 120.43 (CH, CH_3-C_6H_4), 123.08 (CF_3), 125.77 (2×CH, CF_3-C_6H_4), 125.90 (CH, C_6H_5), 128.53 (CH, C_6H_5), 129.08 (2×CH, C_6H_5), 129.43 (2×CH, CH_3-C_6H_4), 131.44 (C, CH_3-C_6H_4), 135.03 (C, thiazole), 137.69 (C, C_6H_5), 137.93 (C, CH_3-C_6H_4), 141.87 (C, CF_3-C_6H_4), 155.01 (C, thiazole), 158.69 (C, thiadiazine), 160.30 (C, thiazole), 162.42 (C, thiadiazine)

5-(4-Phenyl-2-(phenylamino)thiazol-5-yl)-*N*-(p-tolyl)-6*H*-1,3,4-thiadiazin-2-amine (6c)

Final compound **6c** was synthesized using starting material *N*-(p-tolyl)hydrazinecarbothioamide **3c** and 2-chloro-1-(4-phenyl-2-(phenylamino)thiazol-5-yl)ethanone **5b** as described in general procedure C. Yellow solid; Yield: 73%; Purity: 98.7%; Melting point: 161-163 °C; Molecular formula: $C_{25}H_{21}N_5S_2$; LC-ESI-MS (m/z): 456.1 $[M+H]^+$; IR (KBr, cm^{-1}): 3142.04, 2924.09, 1598.99, 771.53; ^{1}H NMR (400MHz, DMSO-d_6) δ: 2.252 (s, 3H, CH_3), 3.238 (s, 2H, CH_2), 6.995-7.098 (m, 5H, C_6H_5 & C_6H_5), 7.337 (d, J = 7.6 Hz, 4H, CH_3-C_6H_4), 7.464-7.478 (m, 1H, C_6H_5), 7.596 (d, J = 6 Hz, 2H, C_6H_5), 7.673 (d, J = 7.6 Hz, 2H, C_6H_5), 10.489 (s, D_2O exchangeable, 1H, NH linked to thiadiazine), 10.552 (s, D_2O exchangeable, 1H, NH linked to thiazole); ^{13}C NMR (400 MHz, DMSO-d_6) δ: 20.39 (CH_3), 29.38 (CH_2), 116.31 (2×CH, CH_3-C_6H_4), 117.42 (2×CH, CH_3-C_6H_4), 118.17 (CH, C_6H_5), 121.90 (CH, C_6H_5), 125.60 (2×CH, C_6H_5), 128.20 (C, CH_3-C_6H_4), 128.48 (2×CH, C_6H_5), 128.95 (2×CH, C_6H_5), 129.04 (CH, C_6H_5), 129.16 (CH, C_6H_5), 139.47 (C, thiazole), 135.22 (C, C_6H_5), 140.51 (C, CH_3-C_6H_4), 141.36 (C, C_6H_5), 152.10 (C, thiazole), 157.32 (C, thiadiazine), 161.04 (C, thiazole), 163.43 (C, thiadiazine)

5-(4-Phenyl-2-(phenylamino)thiazol-5-yl)-*N*-(4-(trifluoromethyl)phenyl)-6*H*-1,3,4-thiadiazin-2-amine (6d)

Final compound **6d** was synthesized using starting material *N*-(4-(trifluoromethyl)phenyl)hydrazinecarbothioamide **3b** and 2-chloro-1-(4-phenyl-2-(phenylamino)thiazol-5-yl)ethanone **5b** as described in general procedure C. Pale yellow solid; Yield: 76%; Purity: 99.0%; Melting point: 183-185 °C; Molecular formula: $C_{25}H_{18}F_3N_5S_2$; LC-ESI-MS (m/z): 510.1 $[M+H]^+$; IR (KBr, cm^{-1}): 3255.84, 2927.94, 1325.10, 771.53, 694.37; ^{1}H NMR (400MHz, DMSO-d_6) δ: 3.281 (s, 2H, CH_2), 7.150 (d, *J* = 7.6 Hz, 2H, CF_3-C_6H_4), 7.479 (t, *J* = 3.2 Hz, 1H, C_6H_5), 7.565 (t, *J* = 5.6 Hz, 2H, C_6H_5), 7.584-7.622 (m, *J* = 5H, C_6H_5 & CF_3-C_6H_4), 7.642 (d, *J* = 8.0 Hz, 2H, C_6H_5), 7.663 (d, *J* = 7.6 Hz, 2H, C_6H_5), 9.780 (s, D_2O exchangeable, 1H, NH linked to thiadiazine), 10.486 (s, D_2O exchangeable, 1H, NH linked to thiazole); ^{13}C NMR (400 MHz, $CDCl_3$) δ: 29.72 (CH_2), 119.80 (2×CH, CF_3-C_6H_4), 120.49, (2×CH, C_6H_5), 120.75 (CH, C_6H_5), 122.19 (2×CH, CF_3-C_6H_4), 124.35 (2×CH, C_6H_5), 125.42 (CF_3), 126.07 (2×CH, C_6H_5), 128.71 (C, CF_3-C_6H_4), 129.19 (CH, C_6H_5), 129.41 (CH, C_6H_5), 129.56 (CH, C_6H_5), 129.69 (C, thiazole), 130.02 (C, C_6H_5), 140.91 (C, C_6H_5), 141.24 (C, CF_3-C_6H_4), 158.46 (C, thiazole), 161.38 (C, thiadiazine), 168.23 (C, thiazole), 170.30 (C, thiadiazine)

***N*-phenyl-5-(4-phenyl-2-(phenylamino)thiazol-5-yl)-6*H*-1,3,4-thiadiazin-2-amine (6e)**

Final compound **6e** was synthesized using starting material *N*-phenylhydrazinecarbothioamide **3d** and 2-chloro-1-(4-phenyl-2-(phenylamino)thiazol-5-yl)ethanone **5b** as described in general procedure C. Yellow solid; Yield: 69%; Purity: 99.3%; Melting point: 169-171 °C; Molecular formula: $C_{24}H_{19}N_5S_2$; LC-ESI-MS (m/z):

442.1 $[M+H]^+$; IR (KBr, cm^{-1}): 3319.49, 2926.01, 1247.94, 771.53; ^1H NMR (400MHz, DMSO-d_6) δ: 3.281 (s, 2H, CH_2), 7.152 (d, *J* = 7.6 Hz, 2H, C_6H_5), 7.468 (t, *J* = 5.6 Hz, 2H, C_6H_5), 7.520 (t, *J* = 7.6 Hz, 4H, C_6H_5), 7.543-7.588 (m, 3H, C_6H_5), 7.631 (d, *J* = 8.0 Hz, 2H, C_6H_5), 7.667 (d, *J* = 7.2 Hz, 2H, C_6H_5), 10.501 (s, D_2O exchangeable, 2H, 2×NH); ^{13}C NMR (400 MHz, $CDCl_3$) δ: 26.93 (CH_2), 118.50 (CH, C_6H_5), 118.81 (CH, C_6H_5), 119.47 (CH, C_6H_5), 120.05 (CH, C_6H_5), 120.51 (CH, C_6H_5), 121.16 (CH, C_6H_5), 121.58 (CH, C_6H_5), 123.55 (CH, C_6H_5), 124.00 (CH, C_6H_5), 128.40 (CH, C_6H_5), 128.58 (CH, C_6H_5), 128.64 (CH, C_6H_5), 128.73 (CH, C_6H_5), 129.21 (CH, C_6H_5), 129.28 (CH, C_6H_5), 129.47 (C, thiazole), 129.64 (C, C_6H_5), 129.99 (C, C_6H_5), 134.22 (C, C_6H_5), 139.86 (C-thiazole), 151.23 (C-thiadiazine), 160.74 (C-thiazole), 162.23 (C-thiadiazine)

_N_-(4-fluorophenyl)-5-(2-((4-fluorophenyl)amino)-4-phenylthiazol-5-yl)-6_H_-1,3,4-thiadiazin-2-amine (6f)

Final compound **6f** was synthesized using starting material *N*-(4-fluorophenyl)hydrazinecarbothioamide **3e** and 2-chloro-1-(2-((4-fluorophenyl)amino)-4-phenylthiazol-5-yl)ethanone **5c** as described in general procedure C. Yellow solid; Yield: 72%; Purity: 99.8%; Melting point: 181-183 °C; Molecular formula: $C_{24}H_{17}F_2N_5S_2$; LC-ESI-MS (m/z): 478.0 $[M+H]^+$; HRMS (TOF) *m/z* calcd for $C_{24}H_{17}F_2N_5S_2$ $[M+H]^+$ 478.0893, found: 478.0698; IR (KBr, cm^{-1}): 3240.11, 2908.65, 1508.33, 769.60; ^1H NMR (400MHz, DMSO-d_6) δ: 3.456 (s, 2H, CH_2), 7.180 (t, *J* = 7.6 Hz, 2H, C_6H_5), 7.208 (d, *J* = 5.6 Hz, 2H, F-C_6H_4), 7.225-7.681 (m, 7H, F-C_6H_4 & C_6H_5), 7.6985 (d, *J* = 7.6 Hz, 2H, C_6H_5), 10.891 (s, D_2O exchangeable, 2H, 2×NH); ^{13}C NMR (400 MHz, $CDCl_3$) δ: 24.47 (CH_2), 115.72 (2×CH, F-C_6H_4), 115.79 (CH, F-C_6H_4), 116.28 (CH, F-C_6H_4), 116.50 (CH, C_6H_5), 120.35 (2×CH, F-C_6H_4), 121.88 (CH, C_6H_5), 122.20 (CH, C_6H_5), 123.09 (CH, C_6H_5), 123.81 (CH, C_6H_5),

128.33 (C, thiazole), 128.66 (C, C_6H_5), 128.80 (C, F-C_6H_4), 128.96 (C, F-C_6H_4), 129.19 (C, thiazole), 134.61 (C, F-C_6H_4), 137.02 (C, F-C_6H_4), 157.48 (C, thiadiazine), 158.77 (C, thiazole), 183.66 (C, thiadiazine)

5-(2-((4-Fluorophenyl)amino)-4-phenylthiazol-5-yl)-*N*-(p-tolyl)-6*H*-1,3,4-thiadiazin-2-amine (6g)

Final compound **6g** was synthesized using starting material *N*-(p-tolyl)hydrazinecarbothioamide **3c** and 2-chloro-1-(2-((4-fluorophenyl)amino)-4-phenylthiazol-5-yl)ethanone **5c** as described in general procedure C. Yellow solid; Yield: 74%; Purity: 99.9%; Melting point: 194-196 °C; Molecular formula: $C_{25}H_{20}FN_5S_2$; LC-ESI-MS (m/z): 474.1 $[M+H]^+$; HRMS (TOF) *m/z* calcd for $C_{25}H_{20}FN_5S_2$ $[M+H]^+$ 474.1144, found: 474.1178; IR (KBr, cm^{-1}): 3352.28, 2914.44, 1546.91, 800.12, 765.41; ^1H NMR (400MHz, DMSO-d_6) δ: 1.992 (s, 3H, CH_3), 3.461 (s, 2H, CH_2), 7.168 (d, J = 7.6 Hz, 2H, CH_3-C_6H_4), 7.203 (t, J = 8.8 Hz, 2H, C_6H_4), 7.468-7.511 (m, 5H, C_6H_5, CH_3-C_6H_4, F-C_6H_4), 7.611-7.628 (m, 2H, F-C_6H_4), 7.644-7.678 (m, 2H, C_6H_5), 10.521 (s, D_2O exchangeable, 1H, NH linked to thiadiazine), 10.910 (s, D_2O exchangeable, 1H, NH linked to thiazole); ^{13}C NMR (400 MHz, DMSO-d_6) δ: 28.51 (CH_3), 30.38 (CH_2), 115.62 (2×CH, CH_3-C_6H_4), 115.84 (2×CH, F-C_6H_4), 119.91 (CH, F-C_6H_4), 119.99 (CH, F-C_6H_4), 124.18 (2×CH, C_6H_5), 124.66 (CH, C_6H_5), 128.18 (2×CH, C_6H_5), 128.66 (2×CH, C_6H_5), 129.24 (C, CH_3-C_6H_4), 129.47 (C, thiazole), 135.20 (C, C_6H_5), 136.35 (2×C, F-C_6H_4 & CH_3-C_6H_4) 156.53 (C-thiazole), 157.17 (C, F-C_6H_4), 158.91 (C, thiadiazine), 165.35 (C, thiazole), 189.57 (C, thiadiazine)

5-(4-Phenyl-2-(phenylamino)thiazol-5-yl)-6*H*-1,3,4-thiadiazin-2-amine (8a)

Final compound **8a** was synthesized using readily available starting material hydrazinecarbothioamide **7a** and 2-chloro-1-(4-phenyl-2-(phenylamino)thiazol-5-yl)ethanone **5b** as described in general procedure C. Yellow solid; Yield: 70%; Purity: 99.7%; Melting point: 193-195 °C; Molecular formula: $C_{18}H_{15}N_5S_2$; LC-ESI-MS (m/z): 366.1 $[M+H]^+$; IR (KBr, cm^{-1}): 3267.41, 3190.26, 2926.01, 771.53 ; ^1H NMR (400MHz, $CDCl_3$) δ: 3.618 (s, 2H, CH_2), 6.907 (t, *J* = 7.6 Hz, 1H, C_6H_5), 7.118 (t, *J* = 6.8 Hz, 2H, C_6H_5), 7.113-7.329 (m, 3H, C_6H_5), 7.341 (d, *J* = 6.8 Hz, 2H, C_6H_5), 7.583 (d, *J* = 8.0 Hz, 2H, C_6H_5), 8.531 (s, D_2O exchangeable, 2H, NH_2), 10.599 (s, D_2O exchangeable, 1H, NH); ^{13}C NMR (400 MHz, $CDCl_3$) δ: 24.94 (CH_2), 108.17 (CH, C_6H_5), 115.89 (2×CH, C_6H_5), 116.23 (2×CH, C_6H_5), 116.38 (CH, C_6H_5), 120.88 (CH, C_6H_5), 121.36 (CH, C_6H_5), 127.20 (CH, C_6H_5), 128.12 (CH, C_6H_5), 128.93 (C-thiazole), 135.44 (C, C_6H_5), 136.87 (C, C_6H_5) 141.56 (C, thiazole), 148.13 (C-thiadiazine), 163.91 (C-thiazole), 168.19 (C-thiadiazine)

5-(2-((4-Fluorophenyl)amino)-4-phenylthiazol-5-yl)-6*H*-1,3,4-thiadiazin-2-amine (8b)

Final compound **8b** was synthesized using starting material hydrazinecarbothioamide and 2-chloro-1-(2-((4-fluorophenyl)amino)-4-phenylthiazol-5-yl)ethanone **5c** as described in general procedure C. Yellow solid; Yield: 71%; Purity: 99.8%; Melting point: 215-217 °C; Molecular formula: $C_{18}H_{14}FN_5S_2$; LC-ESI-MS (m/z): 384.1 $[M+H]^+$; HRMS (TOF) *m/z* calcd for $C_{18}H_{14}FN_5S_2$ $[M+H]^+$ 384.0675, found: 384.0824; IR (KBr, cm^{-1}): 3188.33, 3138.18, 2947.23, 1598.99, 835.18, 754.21; ^1H NMR (400MHz, $CDCl_3$) δ: 3.623 (s, 2H, CH_2), 6.932 (t, *J* = 6.4 Hz, 2H, C_6H_5), 7.094-7.128 (m, 2H, C_6H_5), 7.306-7.333 (m, 3H, C_6H_5 & F-C_6H_4), 7.575 (d, *J* = 4.8 Hz, 2H, C_6H_5), 8.529 (s, D_2O exchangeable, 2H, NH_2), 10.489 (s, D_2O exchangeable, 1H, NH); ^{13}C NMR (400 MHz, $CDCl_3$) δ: 25.06 (CH_2), 104.07 (2×CH, F-C_6H_4), 115.92 (2×CH, F-C_6H_4), 116.14 (CH, C_6H_5), 116.73 (CH, C_6H_5), 121.48

(CH, C_6H_5), 121.56 (CH, C_6H_5), 128.25 (CH, C_6H_5), 128.52 (C-thiazole), 129.08 (C, C_6H_5), 135.40 (C, F-C_6H_4), 136.38 (C, thiazole), 142.38 (C, F-C_6H_4), 149.03 (C-thiadiazine), 164.40 (C-thiazole), 168.62 (C-thiadiazine)

5-(2-((4-Chlorophenyl)amino)-4-phenylthiazol-5-yl)-6*H*-1,3,4-thiadiazin-2-amine (8c)

Final compound **8c** was synthesized using starting material hydrazinecarbothioamide **7a** and 2-chloro-1-(2-((4-chlorophenyl)amino)-4-phenylthiazol-5-yl)ethanone **5d** as described in general procedure C. Yellow solid; Yield: 77%; Purity: 99.1%; Melting point: 186-188 °C; Molecular formula: $C_{18}H_{14}ClN_5S_2$; LC-ESI-MS (m/z): 399.5 $[M]^+$, 401.5 $[M+2]^+$; IR (KBr, cm^{-1}): 3452.21, 3310.19, 2957.20, 1508.26, 748.52; ^{1}H NMR (400MHz, DMSO-d_6) δ: 3.329 (s, 2H, CH_2), 6.975 (t, *J* = 7.6 Hz, 2H, C_6H_5), 7.336-7.405 (m, 2H, Cl-C_6H_4), 7.451-7.896 (m, 3H, C_6H_5 & Cl-C_6H_4), 7.939 (d, *J* = 7.6 Hz, 2H, C_6H_5), 8.387 (s, D_2O exchangeable, 2H, NH_2), 10.614 (s, D_2O exchangeable, 1H, NH); ^{13}C NMR (400 MHz, $CDCl_3$) δ: 25.12 (CH_2), 107.13 (2C), 116.01 (2×CH, Cl-C_6H_4), 116.17 (CH, C_6H_5), 116.81 (CH, C_6H_5), 121.43 (CH, C_6H_5), 121.65 (CH, C_6H_5) , 128.11 (C, Cl-C_6H_4), 128.37 (CH, C_6H_5), 129.18 (C-thiazole), 134.26 (C, C_6H_5), 136.52 (C-Cl-C_6H_4), 141.99 (C-thiazole), 148.93 (C-thiadiazine), 164.52 (C-thiazole), 167.86 (C-thiadiazine)

Biological Evaluation

4) In *vitro* BACE-1 inhibition assay

BACE-1 inhibition of the compounds were assayed by fluorimetric method using multimode plate reader (Varioskan® Flash). The assay was performed in black 96-well plates. The assay reaction contained 4.0 ng/µl of human BACE-1, 50 µM substrate (MCA-SEVNLDAEFR-Ednp-KRR-NH_2· 3TFA) and test compounds (dissolved in DMSO) in 0.1 M sodium acetate

buffer (pH 4.5). Compounds were tested using 100, 10 and 1 μM Concentration. Readings were observed just after completion of addition termed as time zero reading using excitation and emission wavelength at 320 nm and 405 nm, respectively. After that, mixture was incubated for 2 hr at 37 °C. Fluorescence measurement was recorded after 2 hr. % inhibition of BACE-1 enzyme and IC_{50} of the compounds were determined.[42] The known Inhibitor AZD3839 was used as a reference molecule with the Ki value of 26.1 nmol/L.[20] Reported values represents mean of 3 determinations ± SEM.

5) *In vivo* study

Animals: Sprague-Dawley rats (either sex, 150–200 g) were housed under standard conditions (Relative humidity: 60 ± 5 %, Temperature: 25 ± 3 °C, 10% air exhaust conditioning unit, 12 hr light/dark cycle, Number of animals: 3 per cage) in the animal house of B. V. Patel PERD Centre, Ahmedabad. Housing and handling of animals were performed in accordance with Good Laboratory Practice (GLP) mentioned in CPCSEA guidelines. All the experiments were conducted after the approval of Institutional Animal Ethics Committee (Approval No: PERD/IAEC/2016/049 & PERD/IAEC/2016/050).

A) Anti-inflammatory activity

1) Carrageenan induced rat paw edema model for acute inflammation: Animals were divided into 13 groups (n=6) denoted as normal control (NC), disease control (DC), positive control (PC) and 10 test compounds (**6a-g & 8a-c**). All the positive control (Diclofenac: 7.5 mg/kg body weight) group animals and test compounds (50 mg/kg body weight) groups animals were pre-dosed orally using a suspension of 0.2% agar. All control group animals received 0.2% agar only. After 1 hr of oral dosing, rat paw edema was induced by subcutaneous injection of 0.1 ml of 1% carrageenan (prepared in normal saline) in the sub

plantar region of left hind paw of each rat. Measurement of paw volume was carried out using mercury plethesmometer. Paw volumes were measured before and 3 hr after the injection of carrageenan. The reduction of edema in treated animals were calculated as percentage (%) edema inhibition using following equation.[21]

% edema inhibition = $(V_t/V_0)_{\text{disease control}} - (V_t/V_0)_{\text{treated}} / (V_t/V_0)_{\text{disease control}}$ X 100

V_t = rat paw volume at 3rd hr

V_0 = rat paw volume at 0th hr

The results obtained are presented as Mean ± SEM (n=6 animals/group) and statistical analysis was performed by one-way ANOVA followed by Tukey's multiple comparision test considering significance level *$p < 0.05$.

2) Formalin induced rat paw edema model for chronic inflammation

Animals were divided into six groups (n=6). For chronic inflammation study, animals were pre dosed with vehicle (normal control), Celecoxib (positive control, 40 mg/kg body weight) and test compounds (50 mg/kg body weight) prepared in 0.2% agar. 0.1 ml of 2% formalin (prepared in normal saline) was injected subcutaneously in the sub plantar region of left hind paw 1 hr after the oral dosing. Dosing was continued for consecutive 5 days. The changes in paw volume were recorded after 5 hr of oral dosing using mercury plethesmometer. % reduction of edema was calculated using following equation.[21]

% edema inhibition = $(V_t/V_0)_{\text{disease control}} - (V_t/V_0)_{\text{treated}} / (V_t/V_0)_{\text{disease control}}$ X 100

V_t = rat paw volume at 5th hr

V_0 = rat paw volume at 0th hr

The results obtained are presented as Mean ± SEM (n=6 animals/group) and statistical analysis was performed by one-way ANOVA followed by Tukey's multiple comparison test considering significance level *p< 0.05.

B) $AlCl_3$ induced model for anti-Alzheimer's activity

Animals were divided into 4 groups (n=6) and predosed orally with test compounds using 0.2 % agar suspension for 28 days: Normal control (normal saline), disease control (normal saline), positive control (Meloxicam, 5mg/kg body weight) and test compound group (50 mg/kg body weight). After oral administration of compounds, animals were injected with aluminium chloride 4.2 mg/kg *i.p.* for 28 days in all the groups except normal control group.[23] Normal control group received vehicle only. Studies were carried out during this 28 days model are described in the following protocols.

a) Behavioral study

Behavioral parameters were observed using elevated plus maze, Y maze and pole climbing apparatus. Training session was given to each animals 5 days before $AlCl_3$ treatment and retention of memory was tested during the 28 days of $AlCl_3$ model.

1) Elevated plus maze test[25]

Elevated plus maze test (EPM) was employed for the evaluation of spatial working memory of rats. The basic principle of EPM is based upon the aversion of animals to heights and open spaces so, they prefer to avoid open spaces and explore closed environment more. This test measures the animal's ability to remember the closed arm location. EPM consisted of two open arms (29 x 5 cm) and two enclosed arms (29 x 5 x 15 cm) connected by central platform (5 x5 cm) elevated at the height of 40 cm from the floor. Training procedure was continued for 5 days and repeated each session after 24 hr, under natural light. In the training

session, each rat was placed in the distal arm of the open maze facing away from central platform and allowed to explore the maze for 5 minutes. During the acquisition session, time required for rat to move from an open arm to enclosed arm known as transfer latency was recorded. Training of animals to this environment shortened the transfer latency time. Total arm entries, enclosed arm entries, open arm entries, % time spent in open arm and % time spent in enclosed arm were also recorded. In the retention session, same procedure was repeated at 7^{th}, 14^{th}, 21^{st} and 28^{th} day of $AlCl_3$ model and transfer latency was recorded. Data was calculated by two-way ANOVA test followed by multiple comparisons of tukey's test (mean ± SEM). Statistical significance was measured as *$p<0.05$ when compared to Normal control and ($^{\#}p<0.05$) when compared to Disease control.

2) Y maze test[26]

This test utilizes the rodent's tendency to explore novel environment. Based on that, immediate working memory can be assessed by Y maze test. This test was used for the evaluation of simultaneous alteration performance (SAP) of the rats. Y maze consisted of 3 identical wooden arms (40 x 9 x 16 cm) placed at 120° with respect to each other. Each rat was placed at the end of one arm and allowed to explore the maze for 5 minutes. Arm entries like A, B and C were recorded visually. SAP was calculated as total number of entries minus two, and the % alteration is calculated as actual correct alteration/maximum alteration x 100. Training was given for consecutive 5 days. % alteration was calculated at 7^{th}, 14^{th}, 21^{st} and 28^{th} day of $AlCl_3$ model.

3) Conditioned Avoidance Response (CAR) rat model[24]

Cook's pole climbing apparatus was used to study the cognitive function of rats. Apparatus had an experimental chamber of 25 x 25 x 25 cm with soundproof enclosure. The grid floor

consisted of metallic bars that conduct electric shock. A pole of 2.5 cm diameter was placed at the center of the apparatus. The study was conducted by placing an animal in the apparatus and allowed to explore the apparatus for 45 sec. Conditioned stimulus using buzzer signal and electric shock i.e. unconditioned stimulus was delivered through grid floor for 45 sec. In the acquisition session animals learned to escape from the foot shock by climbing to pole after buzzer signal. Every rats were trained for 3 days. 1st day 5 trials, 2nd day 3 trials and 3rd day 1 trial was conducted to train the animals. Conditioned avoidance response (CAR) was noted for each rat. During retention session, animals were subjected to 1 trial of CAR at 7th, 14th, 21st and 28th day of $AlCl_3$ model.

b) Estimation of haematological parameters:

After 28 days of treatment, on 29th day blood samples were collected from the retro orbital sinus of rats. Rats were anaesthetized by isoflurane and blood samples were collected in 1 ml heparinized micro centrifuge tubes for further haematological studies. Haemoglobin and haematocrit level were estimated using automated haematology analyser (VetScan HM-5; Abaxis Inc., Union City, CA, USA).[32]

c) Serum biochemical assays:

Rats were anaesthetized under isoflurane and blood samples were collected from retro orbital sinus in 1 ml non-heparinized micro centrifuge tubes. Serum was collected from the blood samples and biochemical parameters like % albumin and total protein was determined by automated analyser (Transasia EM 360).[32]

d) Anti-oxidant activity:

Animals in all the groups were treated for 28 days as per the above treatments. On day 29, all the animals were euthanized and intact brain was removed. Each brain was washed with

saline to remove traces of blood. Brain tissues were further used for the estimation of lipid peroxidase and superoxide dismutase assays.

Lipid peroxidase (LPO) assay[23]

Brain tissues from all the groups were taken and kept into 5 ml of Hank's balanced salt solution (HBSS, pH 7.4). Brain tissues were homogenized using Polytron homogenizer (Kinematica, Switzerland) at 5000 rpm of 3 cycles (30 sec of each cycle). After that, homogenates were centrifuged for 10 min using sorvall, legend X1R centrifuge at 35,000 rpm. Supernatant was discarded in each sample and pellet was re-suspended in 0.1 ml of HBSS and further used for LPO assay. Reaction of malonaldehyde (MDA): thiobarbituric acid (TBA) is used as a measure of LPO activity. The assay reaction contained 0.1 ml of tissue homogenate (as processed earlier), 8.1% of sodium dodecyl sulfate 2 ml, 20% acetic acid 1.5 ml (pH 3.5 was adjusted using 1 M NaOH), and 1.5 ml of 0.8% aqueous solution of TBA. Reaction mixture volume was made up to 4 ml by adding 0.7 ml double distilled water. Reaction mixture was subjected to heating in a water bath for 1 hr at 95 °C. 1 ml of double distilled water and 5 ml of n-butanol: pyridine mixture (15:1 v/v) was added after heating and vortexed for 5 min. Further, reaction mixture was centrifuged for 7 min at 3000 rpm and organic supernatant was taken and processed for MDA calculation. Formation of MDA was measured by using an Ultra violet/Visible Spectrophotometer (Shimadzu UV-1800) at 532 nm. Extinction coefficient of MDA was used for calculation (1.45×10^{-5}/min/cm).

LPO was calculated using following formula:

LPO= [(Sample-Blank)*145]*10^{-5}/weight of organ (grams)

Superoxide dismutase (SOD) assay[43]

Brain tissues were taken in 2 ml of chilled 50 mM Tris buffer (pH 8.2 was adjusted by 2 mM EDTA). Homogenization of 3 cycles of 30 sec was done. The homogenate was treated with 1 ml of 0.1% Triton X 100 (v/v) at 4 °C for 30 min. Reaction mixture was then centrifuged at 4 °C for 30 min at 5600 rpm. Supernatant was used for SOD assay. Supernatant was divided into two parts. One part was stored at 4-8 °C and another part was subjected to heating at 95 °C for 1 hr. SOD observations were taken by adding pyrogallol to each sample. Absorbance readings were taken at 420 nm after 0^{th} and 9^{th} min of pyrogallol addition. All calculations were made in terms of per gram fresh weight. SOD enzyme activity was measured by following equation:

Enzyme activity (Units/mg of fresh tissue weight) = $\Delta B-\Delta E/\Delta P*120$

Where, ΔB = Boiled sample absorbance per min (9^{th} reading – 0^{th} reading)

ΔE = Cold sample absorbance per min (9^{th} reading– 0^{th} reading)

ΔP = Pyrogallol Control per min (9^{th} reading – 0^{th} reading)

e) Histopathological studies of brain samples:

Brain samples were isolated and stored in 10 % neutral buffered formalin solution for 24 hr. Sections of brain tissues were stained by Congo red and haemoatoxylin-eosin (HE). The slides were observed under optical microscope (ProgRes C3 OLYMPUS, U-TV1 X, Japan) and images were taken using Progres capturePro 2.9.0.1 softwre.

f) Gastro-intestinal (GI) safety study of compound 6d:

All the anti-inflammatory compounds showed GI adverse events when given in higher doses.[30] In order to evaluate the GI safety of the test compound, euthanized animals were subjected to GI opening. Abdomens of the animals were opened, stomach and intestines were

washed with cold phosphate buffer saline (0.01M, at pH 7.4) and stored in sterile tubes. Stomach and intestine samples were kept in 10 % neutral buffered formalin for 24 hr. Samples were washed with 70 % ethanol and observed for the haemorrhagic damage. Gastric damage was calculated by digital vernier caliper (Absolute AOS Digimatic; Mitutoyo, Japan) and lesion index was calculated for stomach and intestinal samples. Histopathogical evaluation of stomach and intestinal damage was also done by using HE stain.[32,33]

Supporting Information

Copies of ^{1}H NMR and ^{13}C NMR spectra of compounds **6a-g & 8a-c** are provided in Supporting Information. This material is available free of charge via the internet at http://pubs.acs.org.

Abbreviations

AD, Alzheimer's disease; BACE-1, β-site APP Cleaving Enzyme-1; APP, Amyloid precursor protein; MTDLs, Multitarget-directed ligands; COXs, Cyclooxygenases; LOX, Lipoxygenase; GSK-3β, Glycogen synthase kinase-3β, AChE, Acetylcholinesterase enzyme; BuChE, butyrylcholinesterase enzyme; PPAR-γ, Peroxisome proliferator-activated receptor-γ; LDL, Low density lipoprotein; BBB, Blood brain barrier; HERG, Human Ether-à-go-go-Related Gene; ROS, Reactive oxygen species; LPO, Lipid peroxidation; SOD, Superoxide dismutase; RT, Room temperature; hr, Hour; NC, Normal control; DC, Disease control; PC, Positive control.

Acknowledgements

All authors thank B. V. Patel Pharmaceutical Education and Research Development (PERD) Centre for providing research facilities. SRS and NBP thank NIRMA University for registering as research scholar.

Funding Sources

Authors thank B. V. Patel Pharmaceutical Education and Research Development (PERD) for financial support. SRS thanks DST-INSPIRE, Govt. of India for providing fellowship to carry out research work.

Conflict of Interest

Authors declare no conflict of interest.

Author Contributions

SRS carried out *in silico* studies, synthesis, in *vitro* studies, and in *vivo* studies. DPS (equal) contribution in *in vivo* studies and helped in manuscript preparation. NBP performed HPLC purity determination (support). RDD helped *in vivo* studies and manuscript preparation. DHP helped in (support) synthesis of compounds. VS supervised synthesis of compounds. MN supervised *in vivo* studies. KKV supervised all experiments including design of molecules, *in silico* studies, synthesis, *in vitro* & *in vivo* studies. The manuscript was revised and approved by all authors.

References

(1) Dagher, A., Bleicher, C., Aston, J. a, Gunn, R. N., Clarke, P. B., and Cumming, P. (2001) Reduced dopamine D1 receptor binding in the ventral striatum of cigarette smokers. *Synapse 42*, 48–53.

(2) Silvestri, R. (2008) Boom in the Development of Inhibitors for the Treatment of Alzheimer's Disease. *Med. Res. Rev. 29*, 2, 295-338.

(3) Ghosh, A. K., and Osswald, H. L. (2014) BACE1 (β-secretase) inhibitors for the treatment of Alzheimer's disease. *Chem. Soc. Rev. 43*, 6765–6813.

(4) Cummings, J., Morstorf, T., and Lee, G. (2016) Alzheimer's drug-development pipeline: 2016. *Alzheimer's Dement. Transl. Res. Clin. Interv. 2*, 222–232.

(5) Agis-Torres, A., Sölhuber, M., Fernandez, M., and Sanchez-Montero, J. M. (2014) Multi-Target-Directed Ligands and other Therapeutic Strategies in the Search of a Real Solution for Alzheimer's Disease. *Curr. Neuropharmacol. 12*, 2–36.

(6) Rubio-Perez, J. M., and Morillas-Ruiz, J. M. (2012) A Review: Inflammatory Process in Alzheimer's Disease, Role of Cytokines. *Sci. World J. 2012*, 1–15.

(7) Meraz-Ríos, M. A., Toral-Rios, D., Franco-Bocanegra, D., Villeda-Hernández, J., and Campos-Peña, V. (2013) Inflammatory process in Alzheimer's Disease. *Front. Integr. Neurosci. 7*, 1–15.

(8) Cornec, A. S., Monti, L., Kovalevich, J., Makani, V., James, M. J., Vijayendran, K. G., Oukoloff, K., Yao, Y., Lee, V. M. Y., Trojanowski, J. Q., Smith, A. B., Brunden, K. R., and Ballatore, C. (2017) Multitargeted Imidazoles: Potential Therapeutic Leads for Alzheimer's and Other Neurodegenerative Diseases. *J. Med. Chem. 60*, 5120–5145.

(9) Bajda, M., Guzior, N., Ignasik, M., and Malawska, B. (2011) Multi-Target-Directed Ligands in Alzheimer 's Disease Treatment. *Curr. Med. Chem.* 4949–4975.

(10) Prati, F., Bottegoni, G., Bolognesi, M. L., and Cavalli, A. (2017) BACE-1 inhibitors : from recent single-target molecules to multitarget compounds for Alzheimer 's disease. *J. Med. Chem.* DOI 10.1021/acs.jmedchem.7b00393.

(11) Hong, L. (2000) Structure of the Protease Domain of Memapsin 2 (beta -Secretase) Complexed with Inhibitor. *Science. 290*, 150–153.

(12) Shimizu, H., Tosaki, A., Kaneko, K., Hisano, T., Sakurai, T., and Nukina, N. (2008) Crystal Structure of an Active Form of BACE1, an Enzyme Responsible for Amyloid Protein Production. *Mol. Cell. Biol. 28*, 3663–3671.

(13) Scott, J. D., Li, S. W., Brunskill, A. P. J., Chen, X., Cox, K., Cumming, J. N., Forman, M.,

Gilbert, E. J., Hodgson, R. A., Hyde, L. A., Jiang, Q., Iserloh, U., Kazakevich, I., Kuvelkar, R., Mei, H., Meredith, J., Misiaszek, J., Orth, P., Rossiter, L. M., Slater, M., Stone, J., Strickland, C. O., Voigt, J. H., Wang, G., Wang, H., Wu, Y., Greenlee, W. J., Parker, E. M., Kennedy, M. E., and Stamford, A. W. (2016) Discovery of the 3-Imino-1,2,4-thiadiazinane 1,1-Dioxide Derivative Verubecestat (MK-8931)-A β-Site Amyloid Precursor Protein Cleaving Enzyme 1 Inhibitor for the Treatment of Alzheimer's Disease. *J. Med. Chem. 59*, 10435–10450.

(14) Oehlrich, D., Prokopcova, H., and Gijsen, H. J. M. (2014) The evolution of amidine-based brain penetrant BACE1 inhibitors. *Bioorganic Med. Chem. Lett. 24*, 2033–2045.

(15) Blass, B. (2015) 5‑Aryl-1-imino-1-oxo-[1,2,4]thiadiazines. *ACS Med. Chem. Lett. 6*, 1031–1034.

(16) Franklin, P. X., Pillai, A. D., Rathod, P. D., Yerande, S., Nivsarkar, M., Padh, H., Vasu, K. K., and Sudarsanam, V. (2008) 2-Amino-5-thiazolyl motif: A novel scaffold for designing anti-inflammatory agents of diverse structures. *Eur. J. Med. Chem. 43*, 129–134.

(17) Giri, R. S., Thaker, H. M., Giordano, T., Williams, J., Rogers, D., Sudersanam, V., and Vasu, K. K. (2009) Design, synthesis and characterization of novel 2-(2,4-disubstituted-thiazole-5-yl)-3-aryl-3H-quinazoline-4-one derivatives as inhibitors of NF-κB and AP-1 mediated transcription activation and as potential anti-inflammatory agents. *Eur. J. Med. Chem. 44*, 2184–2189.

(18) Glide, Maestro 11.1.012, Schrödinger, LLC, New York, NY, 2017.

(19) Banion, M. K. O. (1999) COX-2 and Alzheimer's disease : potential roles in inflammation and neurodegeneration. *Expert Opin. Investig. Drugs*. 1521–1536.

(20) Jeppsson, F., Eketjäll, S., Janson, J., Karlström, S., Gustavsson, S., Olsson, L. L., Radesäter,

A. C., Ploeger, B., Cebers, G., Kolmodin, K., Swahn, B. M., Von Berg, S., Bueters, T., and Fälting, J. (2012) Discovery of AZD3839, a potent and selective BACE1 inhibitor clinical candidate for the treatment of alzheimer disease. *J. Biol. Chem. 287*, 41245–41257.

(21) Pillai, A. D., Rathod, P. D., X, F. P., Patel, M., Nivsarkar, M., Vasu, K. K., Padh, H., and Sudarsanam, V. (2003) Novel drug designing approach for dual inhibitors as anti-inflammatory agents: Implication of pyridine template. *Biochem. Biophys. Res. Commun. 301*, 183–186.

(22) Zhang, F., Jiang L. (2014) Neuroinflammation in Alzheimer's disease. *Neuroinflammation Neurodegener.* 161–177.

(23) Parekh, K. D., Dash, R. P., Pandya, A. N., Vasu, K. K., and Nivsarkar, M. (2013) Implication of novel bis-imidazopyridines for management of Alzheimer's disease and establishment of its role on protein phosphatase 2A activity in brain. *J. Pharm. Pharmacol. 65*, 1785–1795.

(24) Wadenberg, M. L. G., and Hicks, P. B. (1999) The conditioned avoidance response test re-evaluated: Is it a sensitive test for the detection of potentially atypical antipsychotics? *Neurosci. Biobehav. Rev. 23*, 851–862.

(25) Liu, L., Orozco, I. J., Planel, E., Wen, Y., Bretteville, A., Krishnamurthy, P., Wang, L., Herman, M., Figueroa, H., Yu, W. H., Arancio, O., and Duff, K. (2008) A transgenic rat that develops Alzheimer's disease-like amyloid pathology, deficits in synaptic plasticity and cognitive impairment *31*, 46–57.

(26) Suo, Z., Cox, A. A., Bartelli, N., Rasul, I., Festoff, B. W., Premont, R. T., and Arendash, G. W. (2007) GRK5 deficiency leads to early Alzheimer-like pathology and working memory impairment. *Neurobiol. Aging 28*, 1873–1888.

(27) Gutierrez, E. R., Arenas, G. M., Trevino, S., Espinosa, B., Chavez, R., Rojas, K., Flores, G., Diaz, A., Guevara, J. (2017) Alzheimer's disease and metabolic syndrome: A link from oxidative stress and inflammation to neurodegeneration. *Synapse.* DOI 10.1002/syn.21990s.

(28) Sultana, R., Cenini, G., and Butterfield, D. A. (2013) Biomarkers of Oxidative Stress in Neurodegenerative Diseases. *Mol. Basis Oxidative Stress*. 359-376.

(29) Casado, A., Encarnacion Lopez-Fernandez, M., Concepcion Casado, M., and de La Torre, R. (2008) Lipid peroxidation and antioxidant enzyme activities in vascular and Alzheimer dementias. *Neurochem Res 33*, 450–458.

(30) Yankner, B. A. (1996) Mechanisms of neuronal degeneration in Alzheimer's disease. *Neuron 16*, 921–932.

(31) Mantyh, P. W., Ghilardi, J. R., Rogers, S., DeMaster, E., Allen, C. J., Stimson, E. R., and Maggio, J. E. (1993) Aluminum, iron, and zinc ions promote aggregation of physiological concentrations of beta-amyloid peptide. *J. Neurochem. 61*, 1171–1174.

(32) Singh, D. P., Borse, S. P. Nvsarkar, M. (2016) A novel model for NSAID induced gastroenteropathy in rats. *J. Pharmacol. Toxicol. Methods. 78*, 66-75.

(33) Singh, D. P., Borse, S. P. Nvsarkar, M. (2017) Co-administration of quercetin with pantoprazole sodium prevents NSAID-induced severe gastroenteropathic damage efficiently: Evidence from a preclinical study in rats. *Exp. Toxicol. Pathol. 69*, 17–26.

(34) Singh, D. P., Borse, S. P. Nvsarkar, M. (2017) Overcoming the exacerbating effects of ranitidine on NSAID-induced small intestinal toxicity with quercetin: Providing a complete GI solution. *Chem. Biol. Interact*. *272*, 53-64.

(35) Eidhoff, U., Zink, F., Hassiepen, U., Ostermann, N., Simic, O., Hommel, U., Worpenberg, S., and Gerhartz, B. (2006) Crystal Structure of Human BACE2 in Complex with a

Hydroxyethylamine Transition-state Inhibitor. *J. Mol. Biol. 355*, 249–261.

(36) Lee, A.Y., Gulnik, S.V., Erickson, J.W. (1998) Conformational switching in an aspartic proteinase. *Nat. Struct. Mol. Bio. 5*, 866-871.

(37) SiteMap, Maestro 11.1.012, Schrödinger, LLC, New York, NY, 2017.

(38) Rimon, G., Sidhu, R. S., Lauver, D. A., Lee, J. Y., Sharma, N. P., Yuan, C., Frieler, R. A., Trievel, R. C., Lucchesi, B. R., and Smith, W. L. (2010) Coxibs interfere with the action of aspirin by binding tightly to one monomer of cyclooxygenase-1. *Proc. Natl. Acad. Sci. 107*, 28–33.

(39) Wang, J. L., Limburg, D., Graneto, M. J., Springer, J., Hamper, J. R. B., Liao, S., Pawlitz, J. L., Kurumbail, R. G., Maziasz, T., Talley, J. J., Kiefer, J. R., and Carter, J. (2010) The novel benzopyran class of selective cyclooxygenase-2 inhibitors. Part 2: The second clinical candidate having a shorter and favorable human half-life. *Bioorganic Med. Chem. Lett. 20*, 7159–7163.

(40) Qikprop, Maestro 11.1.012, Schrödinger, LLC, New York, NY, 2017.

(41) Hullin, R.P.; Miller, J.; Short, W.F. (1947) Amidines. part V. preparation of amidines from cyanides and substituted aminomagnesium halides, *J. Chem. Soc. 12*, 394.

(42) Costanzo, P., Cariati, L., Desiderio, D., Sgammato, R., Lamberti, A., Arcone, R., Salerno, R., Nardi, M., Masullo, M., and Oliverio, M. (2016) Design, Synthesis, and Evaluation of Donepezil-Like Compounds as AChE and BACE-1 Inhibitors. *ACS Med. Chem. Lett. 7*, 470–475.

(43) Marklund, S., Marklund, G. (1974) Involvement of the superoxide anion radical in the autooxidation of pyrogallol and a convenient assay for superoxide dismutase. *Eur J Biochem. 47,* 469–474.

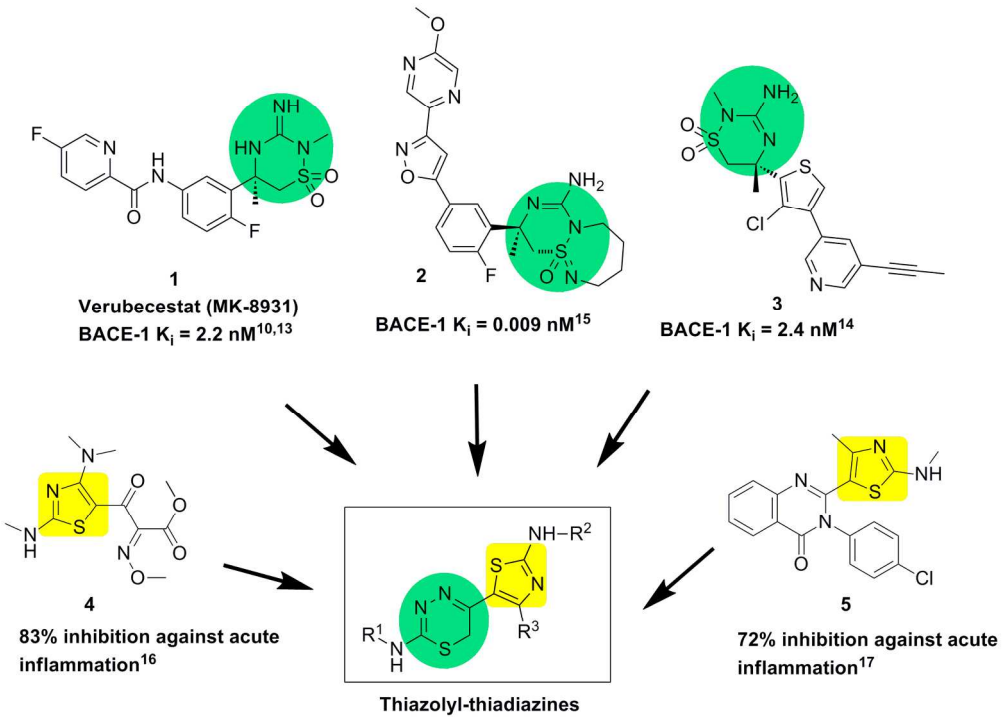

181x130mm (300 x 300 DPI)

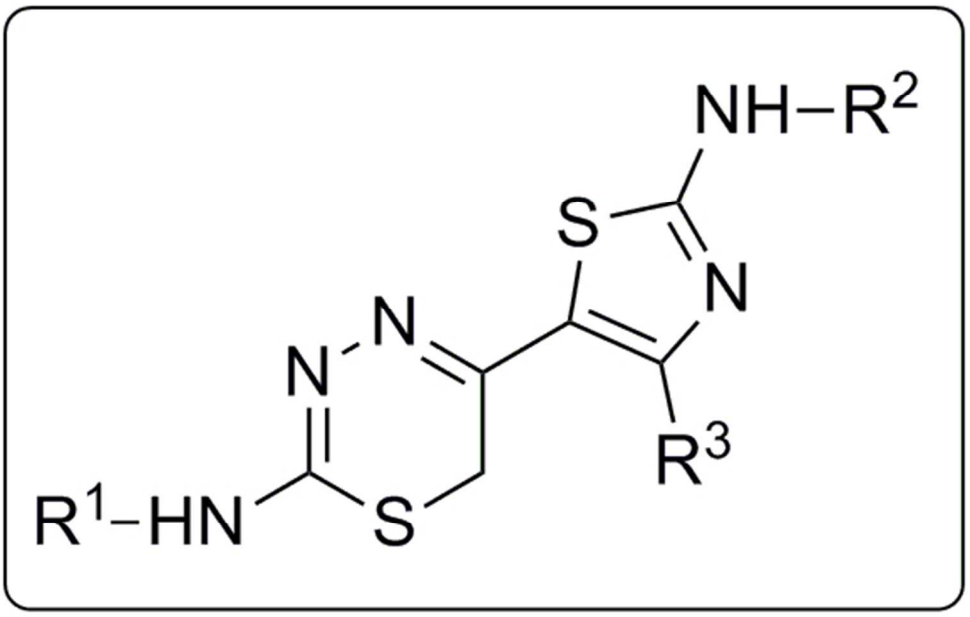

50x32mm (300 x 300 DPI)

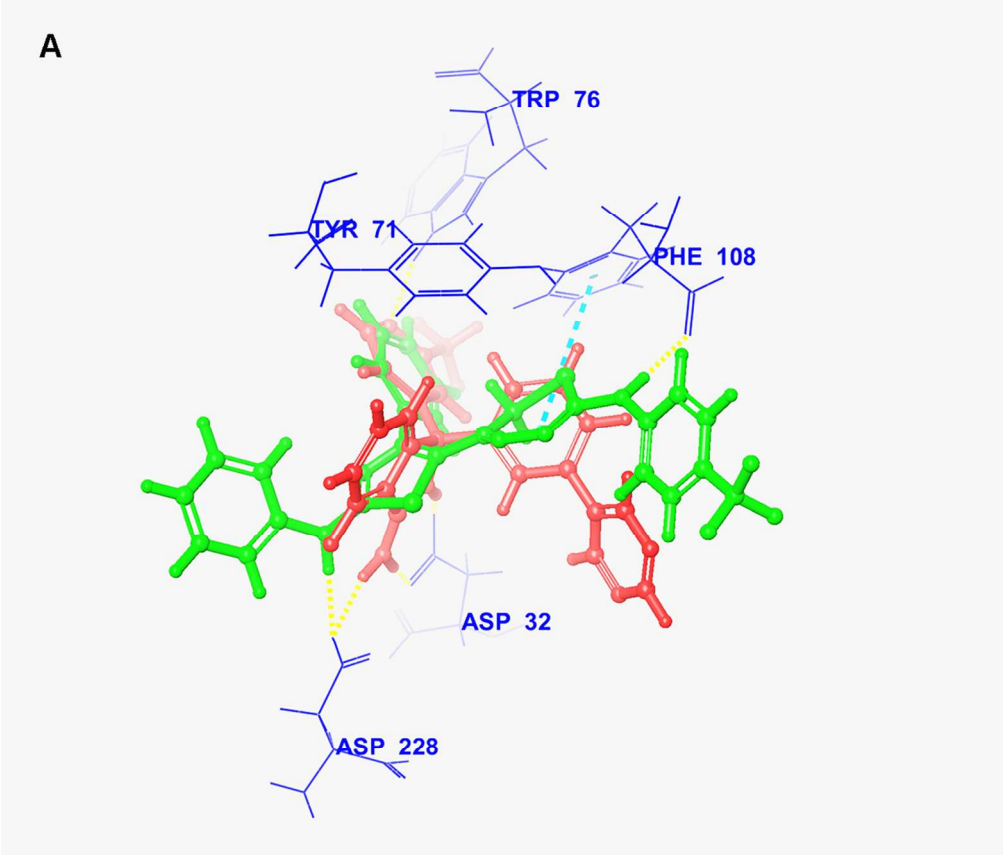

109x93mm (300 x 300 DPI)

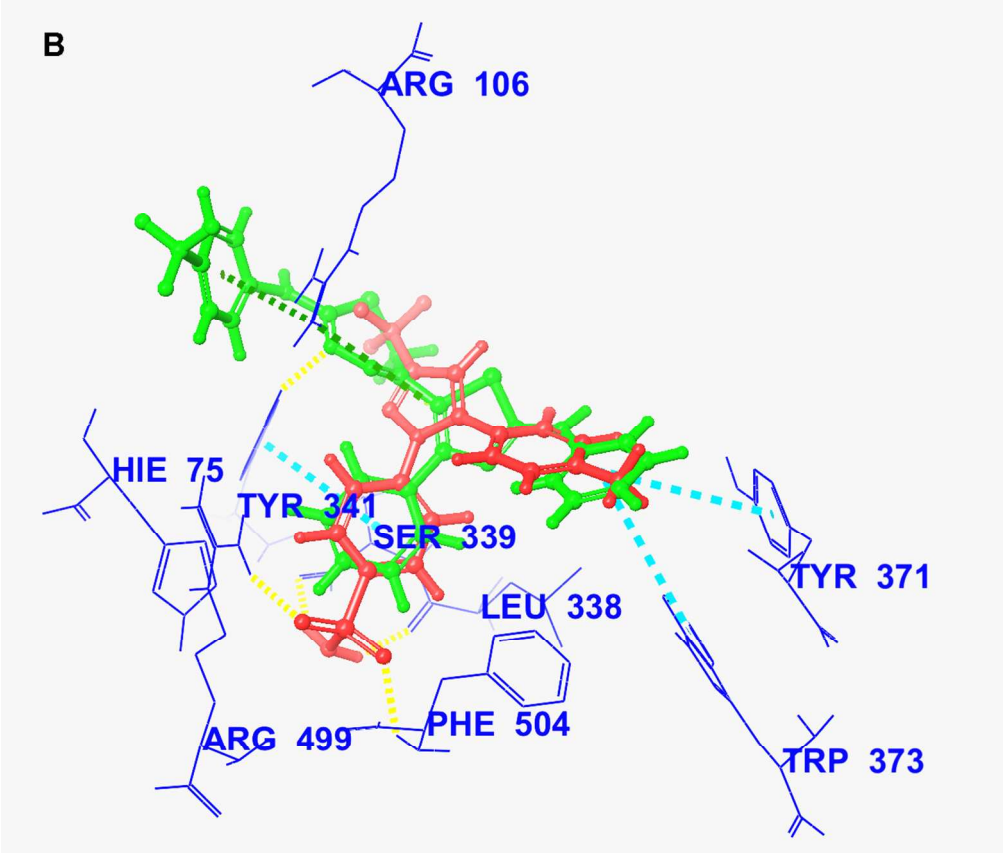

110x93mm (300 x 300 DPI)

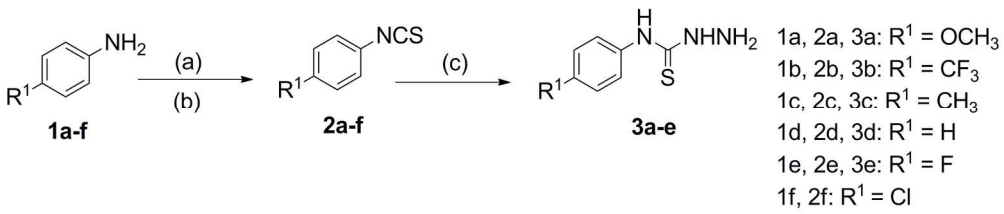

187x39mm (300 x 300 DPI)

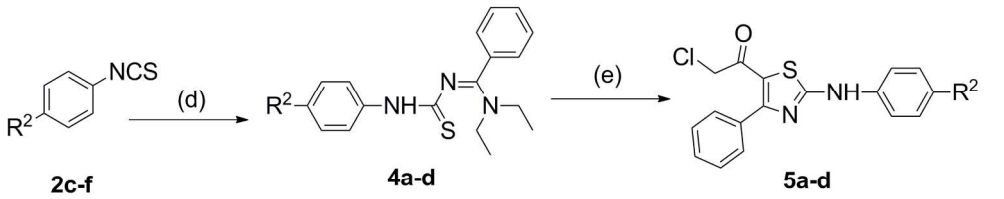

2c, 4a, 5a: $R^2 = CH_3$
2d, 4b, 5b: $R^2 = H$
2e, 4c, 5c: $R^2 = F$
2f, 4d, 5d: $R^2 = Cl$

180x63mm (300 x 300 DPI)

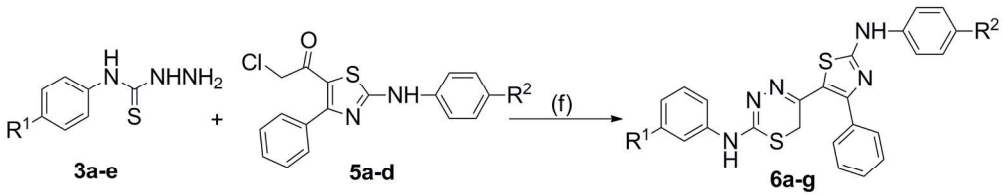

6a: $R^1 = OCH_3$, $R^2 = CH_3$
6b: $R^1 = CF_3$, $R^2 = CH_3$
6c: $R^1 = CH_3$, $R^2 = H$
6d: $R^1 = CF_3$, $R^2 = H$
6e: $R^1 = H$, $R^2 = H$
6f: $R^1 = F$, $R^2 = F$
6g: $R^1 = CH_3$, $R^2 = F$

189x62mm (300 x 300 DPI)

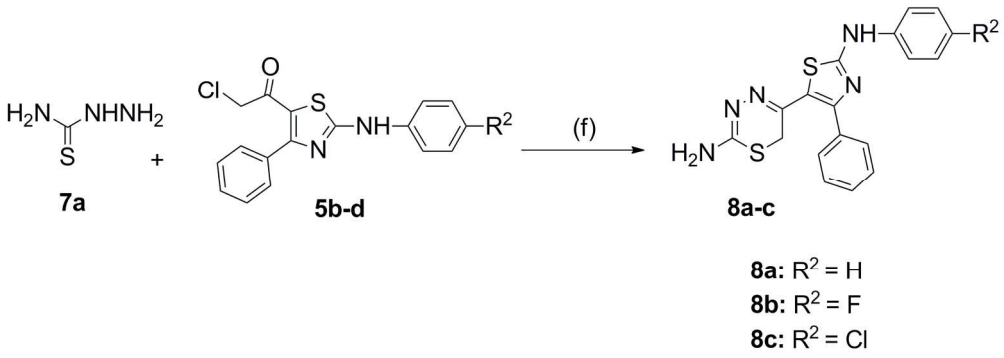

174x62mm (300 x 300 DPI)

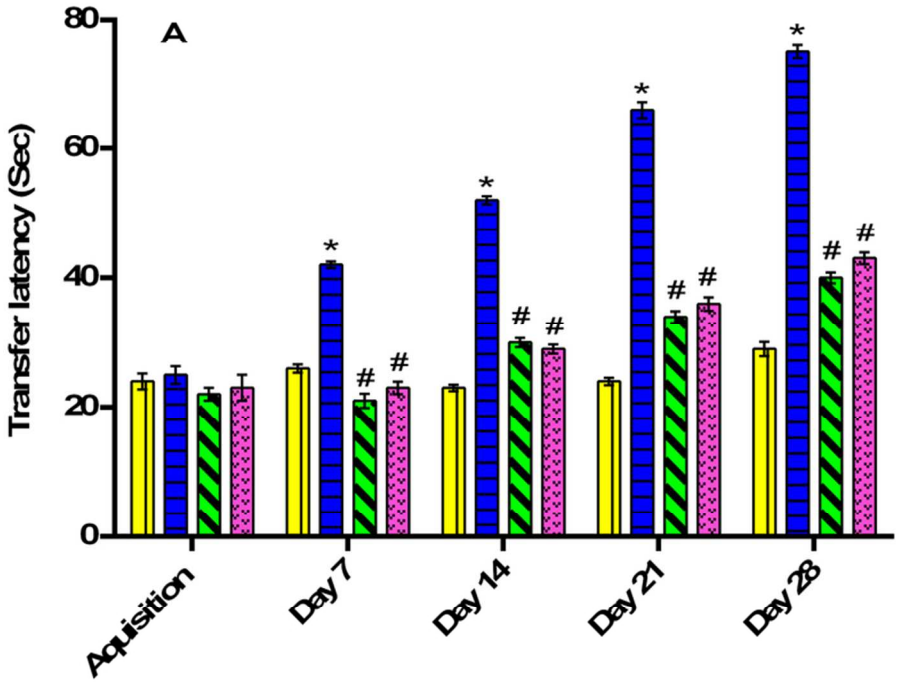

74x55mm (300 x 300 DPI)

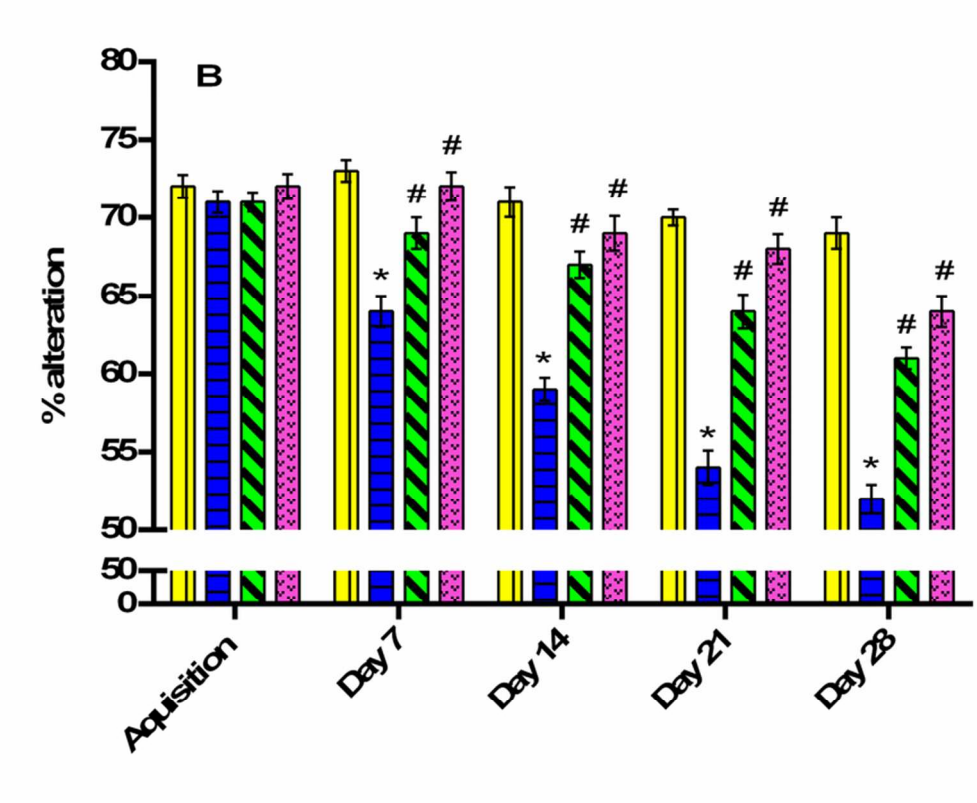

75x60mm (300 x 300 DPI)

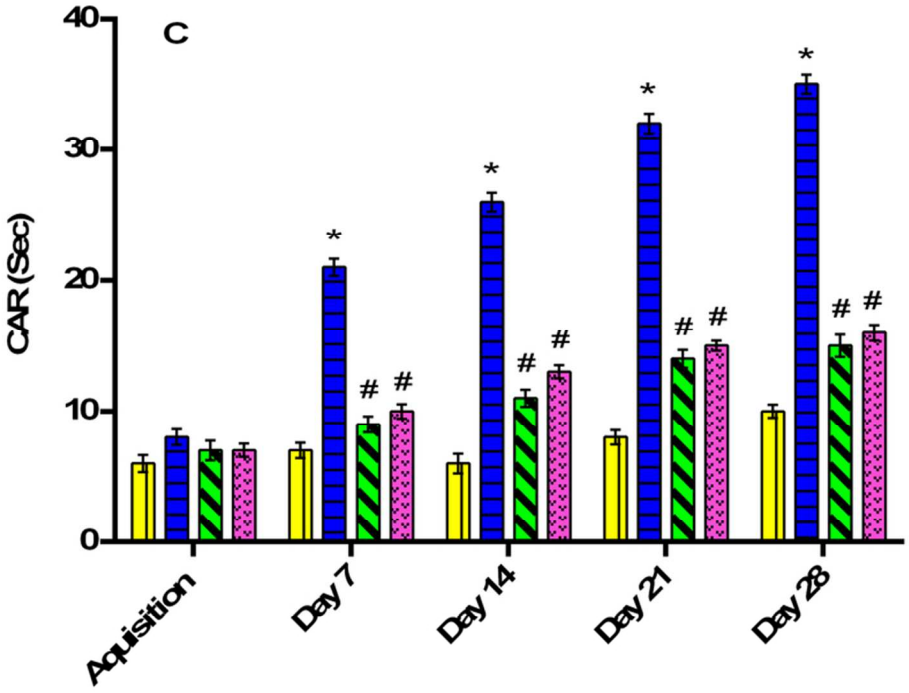

73x55mm (300 x 300 DPI)

40x6mm (300 x 300 DPI)

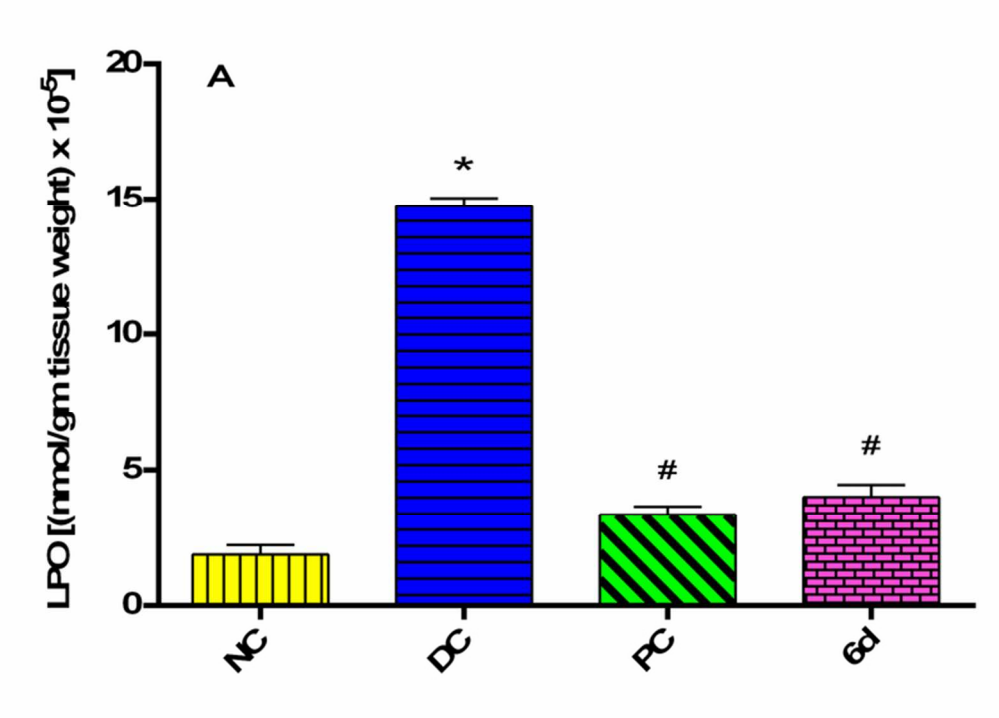

67x48mm (300 x 300 DPI)

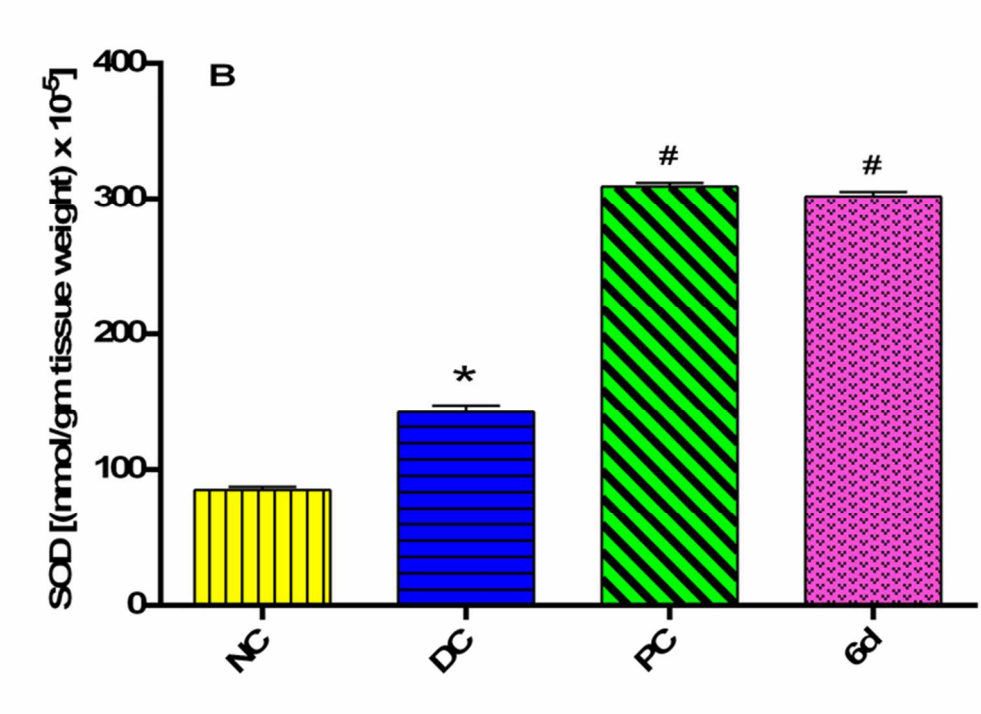

67x48mm (300 x 300 DPI)

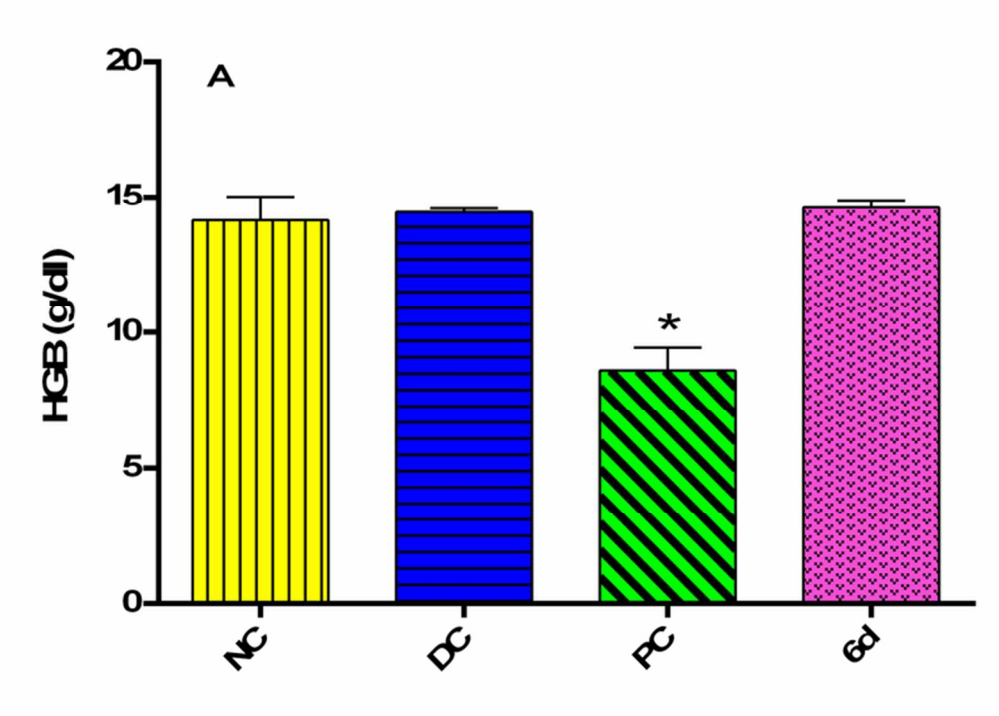

67x48mm (300 x 300 DPI)

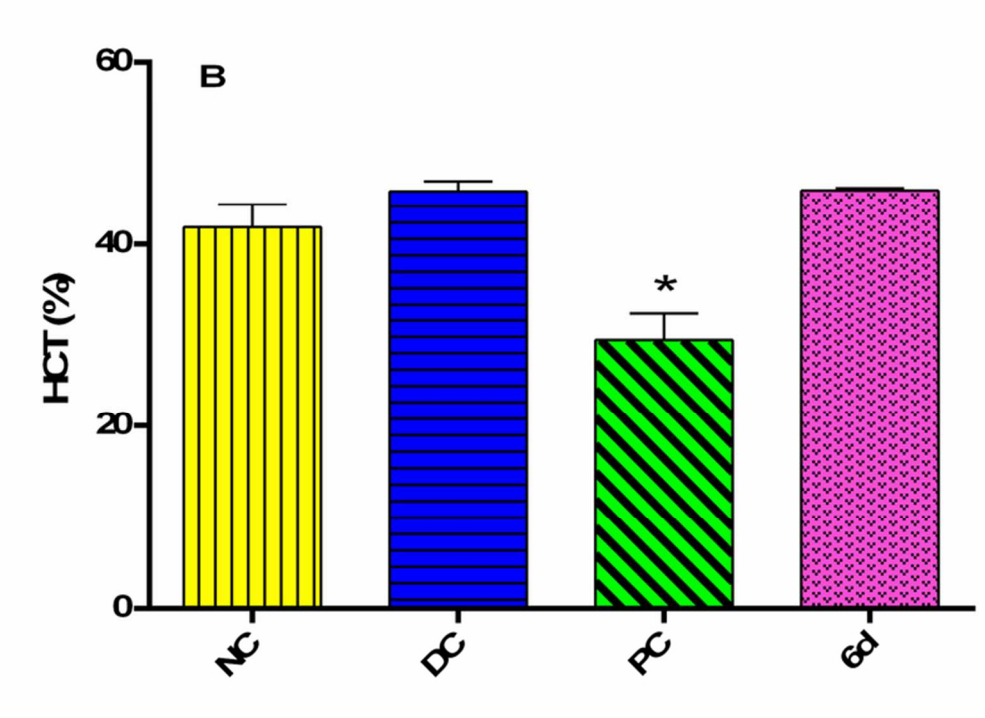

67x49mm (300 x 300 DPI)

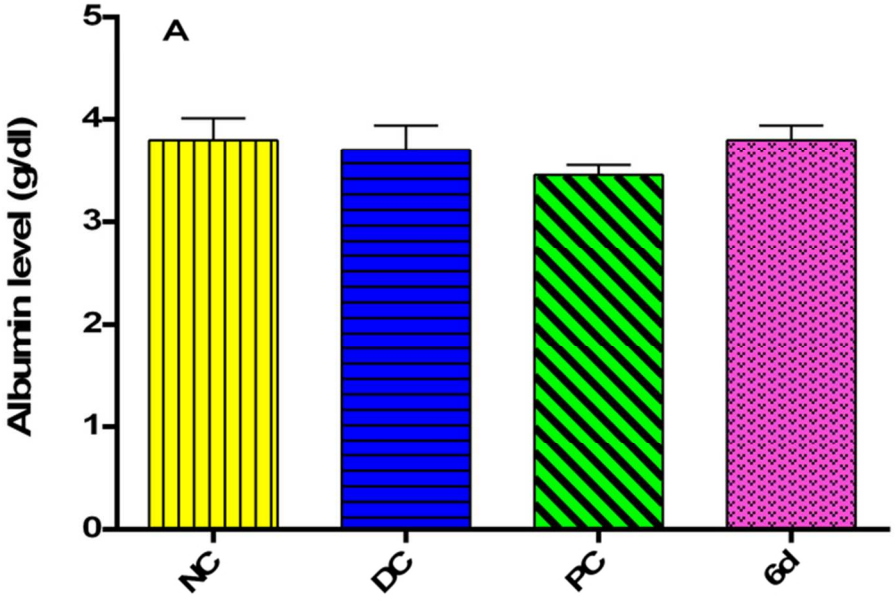

67x46mm (300 x 300 DPI)

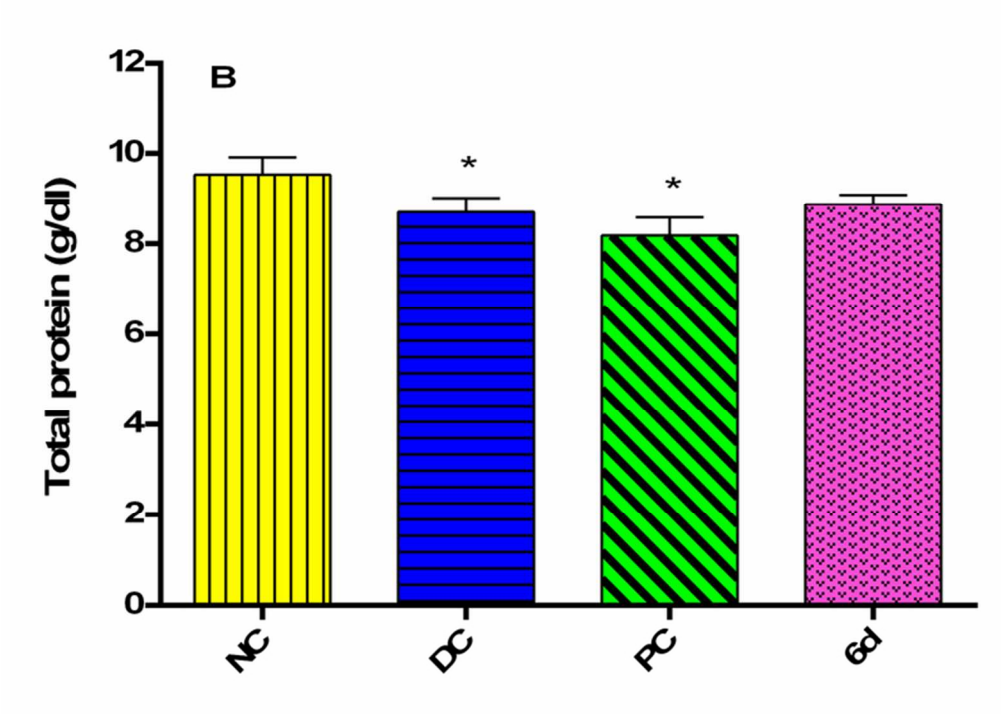

67x48mm (300 x 300 DPI)

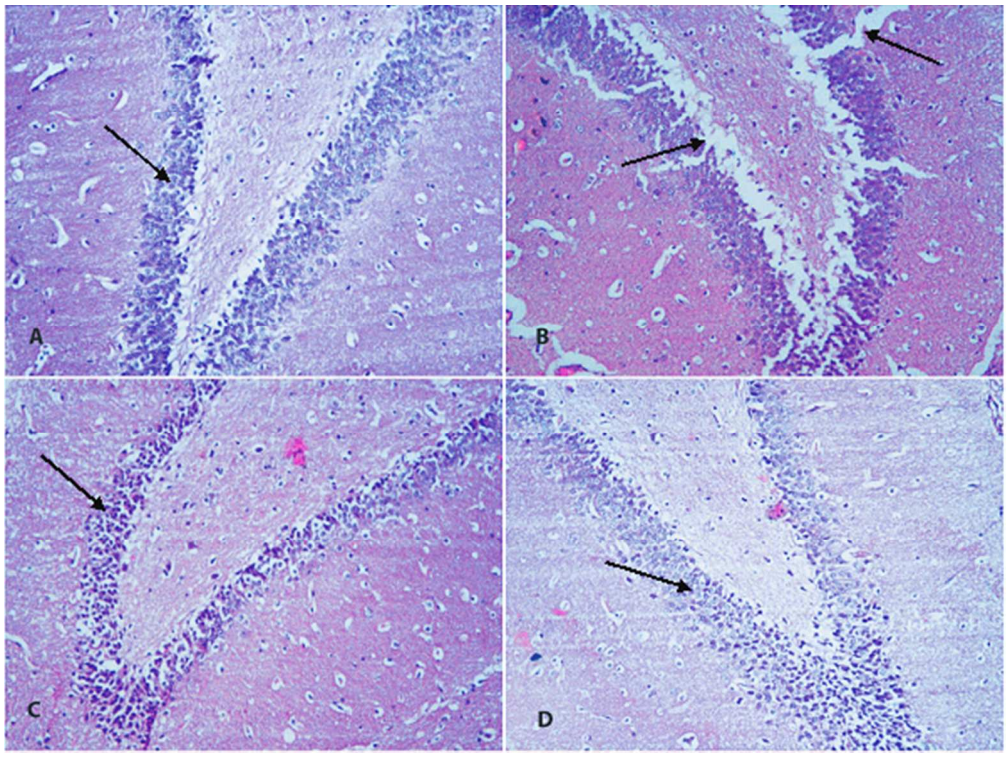

50x37mm (300 x 300 DPI)

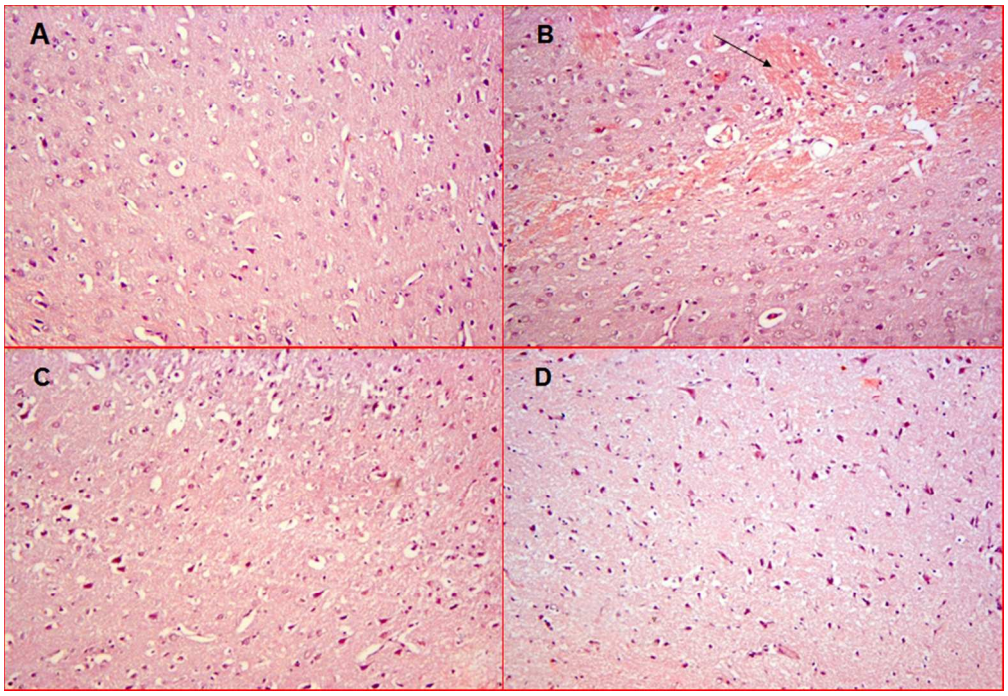

80x54mm (300 x 300 DPI)

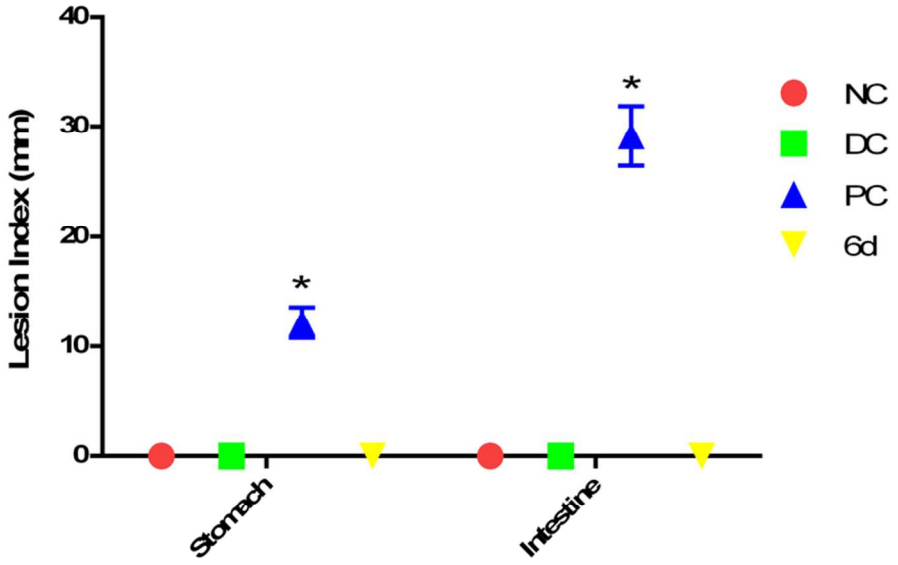

75x48mm (300 x 300 DPI)

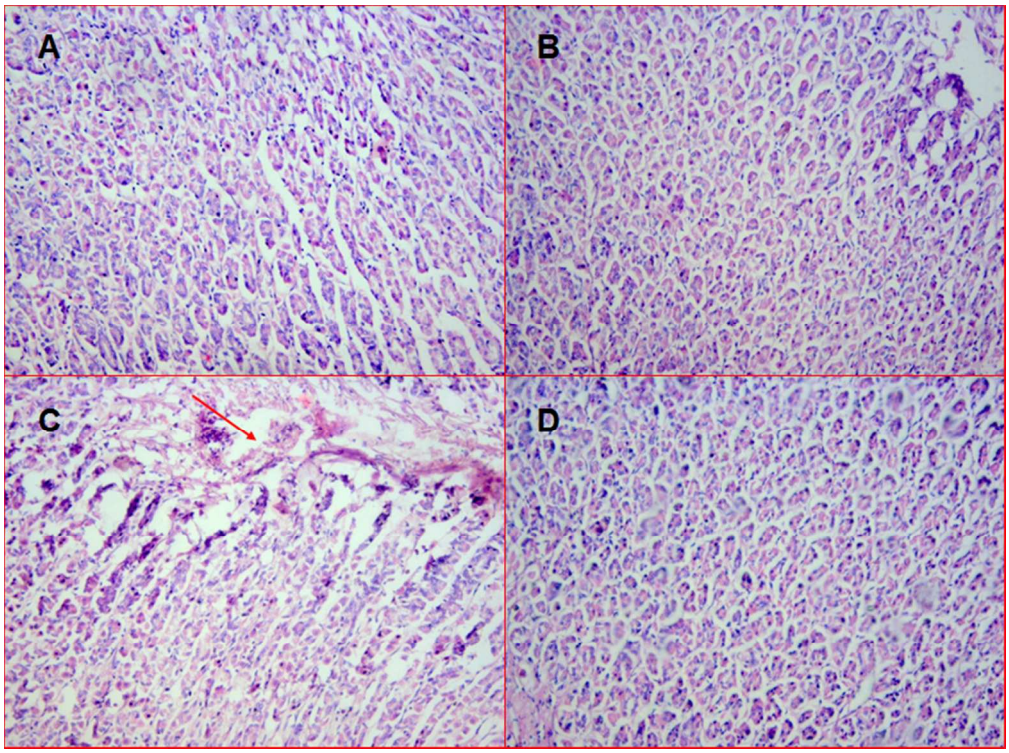

71x53mm (300 x 300 DPI)

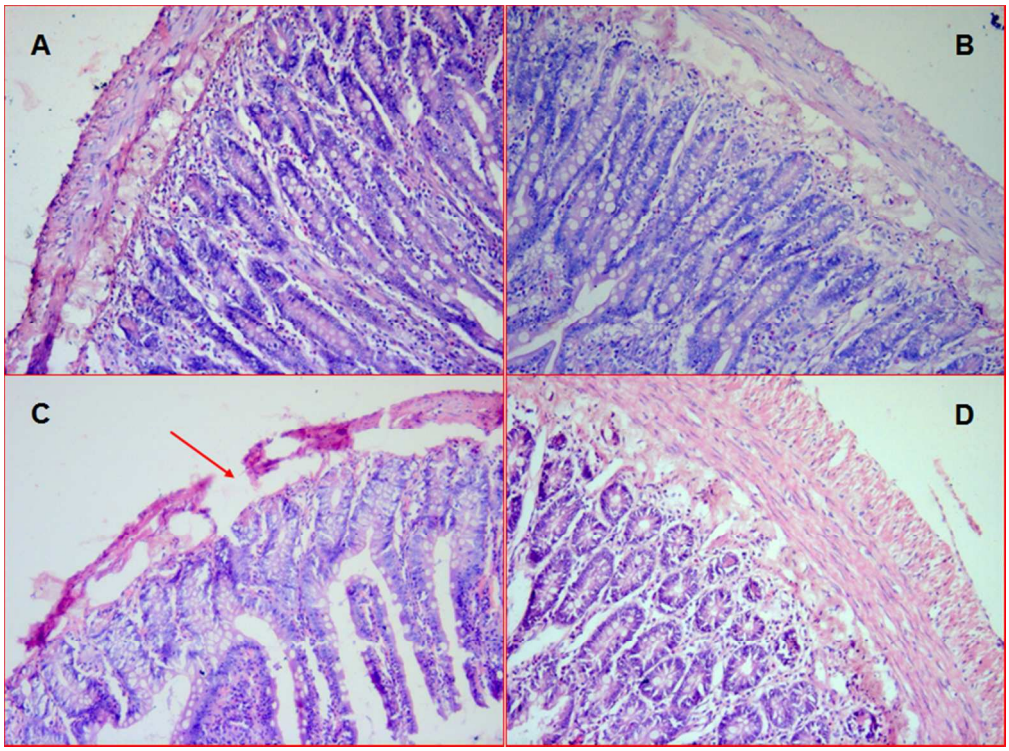

71x53mm (300 x 300 DPI)

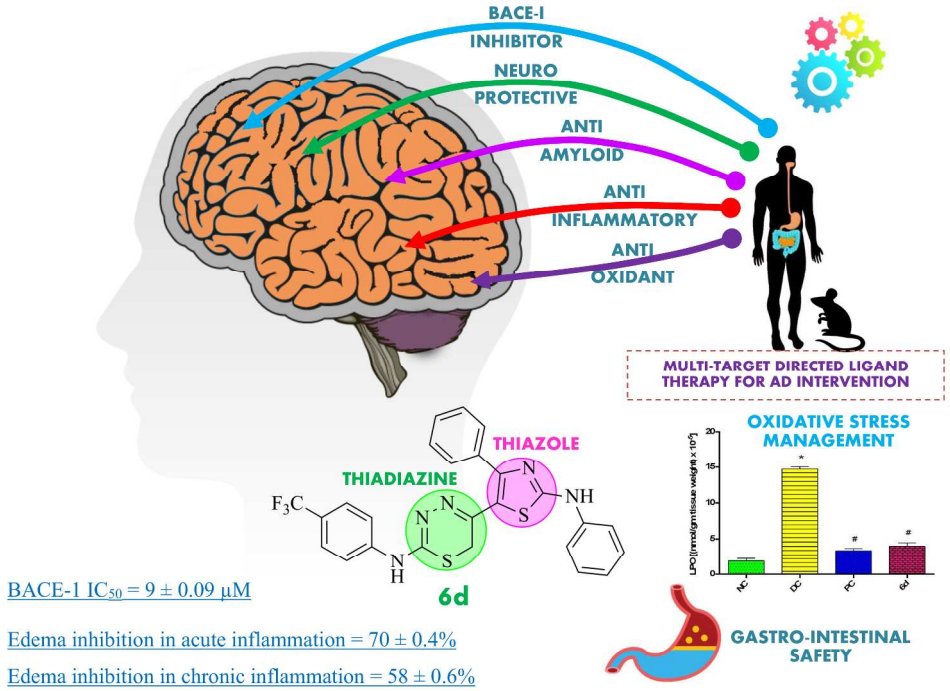

Graphical Abstract

266x201mm (300 x 300 DPI)